UNIVERSITY OF CALIFORNIA

Santa Barbara

A new species of *Pinnarctidion* from the Pysht Formation of Washington and phylogenetic analysis of basal pinnipedimorphs (Eutheria, Carnivora)

A Thesis submitted in partial satisfaction of the
requirements for the degree Master of Science
in Earth Science

by

Christopher John Everett

Committee in charge:
Professor André Wyss, Chair
Professor Susannah Porter
Professor Bruce Tiffney

March 2020

The thesis of Christopher John Everett is approved.

_____

Bruce Tiffney

_____

Susannah Porter

_____

André Wyss, Committee Chair

March 2020

ABSTRACT

A new species of *Pinnarctidion* from the Pysht Formation of Washington and a phylogenetic analysis of basal pinnipedimorphs (Eutheria, Carnivora)

by

Christopher J. Everett

A nearly complete skull and fragmentary postcrania of a late Oligocene pinnipedimorph (SDNHM 146624) from the Pysht Formation of Clallam County, Washington, represent a new species of *Pinnarctidion*, a taxon previously known only from California and Oregon. This study provides a detailed anatomical description of SDNHM 146624 and offers the most comprehensive phylogenetic analysis of early-diverging pinnipedimorphs to date. Notable features of SDNHM 146624 include a posteriorly broad palate coupled with an anteriorly narrow rostrum, dorsoventrally deep zygomatic arches, and accessory cuspules on P3 and P4. The results of extensive comparisons indicate that SDNHM 146624 represents a new species of *Pinnarctidion*, *P. iverseni*, closely related to *P. bishopi* from California. Given the specimen's superb preservation and relative completeness, SDNHM 146624 provides welcome new dental and cranial information for *Pinnarctidion*.

TABLE OF CONTENTS

INTRODUCTION

Various terrestrial mammal lineages have given rise to highly specialized aquatic descendants, each of which is characterized by a unique constellation of features related to swimming, feeding, and reproducing in water. The most highly aquatic mammals, cetaceans and sirenians, essentially never leave the water, while the amphibious "flipper-footed" pinnipeds retain terrestrial locomotory capabilities, sensory acuity in air, and reproduction on land (or ice). Still, many pinnipeds swim and dive as capably as more fully marine mammals (Schreer and Kovacs, 1997).

The three major groups of crown clade pinnipeds include phocid seals, otariid sea lions and fur seals, and odobenid walruses. Each is morphologically and behaviorally distinct, presenting a rich basis for assessing their evolutionary relationships and patterns of character transformation. Two hypotheses regarding the origin of pinnipeds have been proposed. The diphyletic view (Tedford 1976, Repenning et al. 1979, de Muizon 1982b, Barnes 1989, Hunt and Barnes 1994) regards phocids as sharing a close ancestry with Mustelidae (weasels and kin), and otariids plus odobenids (otarioids) as sharing ancestry with Ursidae (bears). This hypothesis requires two separate marine transitions among arctoid carnivorans, along with extensive convergence between these ostensibly distantly related aquatic groups. Although support for diphyly has waned in recent years, some workers continue to advocate separate phocid and otarioid origins on morphological and biogeographical grounds (e.g., Koretsky et al. 2016). By contrast, the monophyletic view of pinniped origins posits that pinnipeds stem from a unique common ancestor from which their aquatic adaptations were inherited. This hypothesis is strongly supported by morphological (Wyss 1987, Wyss and Flynn 1993, Berta and Wyss 1994), immunological (Sarich 1969),

and biomolecular evidence (Arnason et al. 2006, Fulton and Strobeck 2006, Nyakatura and Bininda-Emonds 2012). While agreement on the question of pinniped monophyly is strong, the clade's nearest extant outgroup remains debated. Some studies indicate Ursidae as the likeliest candidate (Wyss and Flynn 1993, Luan et al. 2013), whereas others point to the Mustelidae (Fulton and Strobeck 2006, Nyakatura and Bininda-Emonds 2012).

Although pinnipedimorphs are suggested to have diverged from terrestrial arctoids by the latest Eocene or early Oligocene (Mitchell and Tedford 1973, Higdon et al. 2007), the group is first recorded in sediments of late Oligocene or early Miocene age from the North Pacific (Miyazaki et al. 1994, Deméré et al. 2003). The oldest largely complete undisputed pinnipedimorph (Berta et al. 1989) indicates that many features related to aquatic locomotion were already present by the Oligocene-Miocene transition, including shortening and strengthening of the humerus and femur, and elongation of digit I of the manus and digits I and V of the pes (Wyss 1989). At the same time, stem pinnipeds retained features of the ancestral carnassial dentition related to shearing. The P4 crowns and embrasure pit between P4 and M1 tend to be reduced in later diverging pinnipedimorphs, suggesting a shift in diet. This trend toward dental simplification culminates in the typically homodont conical cheek teeth of crown pinnipeds, which are thought to be consistent with a piercing rather than a shearing or crushing function (Adam and Berta 2001).

Since the first stem pinniped fossil came to light (Mitchell and Tedford 1973), the taxonomy of the group has gone through several iterations. The first specimens were described as various species of *Enaliarctos*, a potentially paraphyletic assemblage long placed within the Enaliarctinae (Mitchell and Tedford 1973). Following the discovery of additional taxa and the establishment of a phylogenetic taxonomic framework (de Queiroz

and Gauthier 1990), the name Pinnipedimorpha was defined as "the most recent common ancestor of *Enaliarctos* [and modern pinnipeds] and all of its descendants" (Berta 1991). This node-based definition would be satisfactory if we could confidently identify the earliest-diverging pinniped relative. However, the evolutionary relationships of the pinniped stem taxa and other early arctoids remain unresolved. The five recognized species of *Enaliarctos* – *E. mealsi* (Mitchell and Tedford 1973), *E. mitchelli* (Barnes 1979), *E. barnesi, E. emlongi,* and *E. tedfordi* (Berta 1991) – were initially considered monophyletic (Berta 1991), but recent work suggests that they constitute multiple genera, and are paraphyletic with respect to crown pinnipeds (Paterson et al. 2020, this study). Other stem-pinnipeds include *Pteronarctos goedertae* (Barnes 1989, Berta 1994b), *Pinnarctidion bishopi* (Barnes 1979), *Pinnarctidion rayi* (Berta 1994a), and *Pacificotaria hadromma* (Barnes 1992). Two superficially otter-like taxa, *Potamotherium valletoni* and *Puijila darwini*, have been interpreted as basal pinnipedimorphs (Rybczynski et al. 2009, Paterson et al. 2020), though it is not certain whether their supposed synapomorphies represent homology or homoplasy among basal arctoids. Due to the unresolved state of the pinniped stem, I propose defining Pinnipedimorpha as a stem-based name that applies to all arctoid carnivorans more closely related to *Phoca vitulina* Linnaeus 1758 than to *Mustela erminea* Linnaeus 1758, *Ursus arctos* Linnaeus 1758, *Ailurus fulgens* Cuvier 1825, or *Procyon lotor* Linnaeus 1758.

The phylogeny of early pinnipedimorphs has received considerable attention (Tedford 1976, Barnes 1989, Berta 1991, Berta and Wyss 1994, Berta et al. 2018, Boessenecker and Churchill 2018). Most previous analyses, however, have focused on relationships within crown Pinnipedia, or have included only a subset of the stem forms. Clearly a more

comprehensive assessment of basal pinnipedimorph relationships is needed to elucidate patterns of character transformation within the group.

Herein I provide a systematic description of a new pinnipedimorph specimen (San Diego Natural History Museum – SDNHM 146624, see Figures 1–5) recovered from the upper levels of the Pysht Formation in Clallam County, Washington, strata considered late Oligocene-early Miocene in age (Prothero et al., 2001). The specimen includes a cranium, cervical vertebra, right humerus, and fragmentary ribs. The well-preserved ventral aspect of the skull and teeth augments the limited record of early pinnipedimorphs in important ways. A craniodentally-based analysis of pinnipedimorph phylogenetic relationships, with an emphasis on the affinities of SDNHM 146624 is also presented.

METHODS

The specimen was prepared by the author primarily at the San Diego Natural History Museum, using mechanical and chemical techniques. Bulk matrix was removed using a PaleoTools PaleoAro pneumatic air scribe. The calcareous siltstone matrix was dissolved in 5% formic acid (HCO_2H) with minimal damage to the fossil. Additional detail was achieved using PaleoTools pin vice and Micro Jack tools. The polymer-based consolidant Paraloid B-72 was used to protect the specimen during chemical preparation and to repair fractures.

Anatomical terminology follows that of Mitchell and Tedford (1973), Barnes (1979), and Berta (1991). Measurements (Table 1) were taken at the LACM and the UCMP using digital calipers following the protocol of Sivertsen (1954) and Barnes (1972).

Institutional Abbreviations—LACM, Natural History Museum of Los Angeles County, Los Angeles, CA; MVZ, Museum of Vertebrate Zoology, University of California, Berkeley; SDNHM, San Diego Natural History Museum, San Diego, CA; UCMP, Museum of Paleontology, University of California, Berkeley, CA; USNM, National Museum of Natural History, Smithsonian Institution, Washington, D.C.; UWBM, University of Washington Burke Museum, Seattle, WA.

I. Systematic Paleontology and Morphological Description of SDNHM 146624

SYSTEMATIC PALEONTOLOGY

EUTHERIA Huxley, 1880

CARNIVORA Bowditch, 1821

ARCTOIDEA Flower, 1869

PINNIPEDIMORPHA Berta el al., 1989

PINNARCTIDION Barnes, 1979

Type species—*Pinnarctidion bishopi* Barnes, 1979.

Included species—*P. bishopi* Barnes, 1979, *P. rayi* Berta, 1994a, and *P. iverseni*, sp. nov.

Occurrence—*P. bishopi* is known from a single specimen (UCMP 86334) collected by Richard C. Bishop from the upper concretion-bearing bed of the Pyramid Hill Sand Member of the Jewett Sand Formation, near Bakersfield, California (UCMP locality V6916

= LACM 1628). *P. rayi* is known from several specimens (USNM 314325, 250321, 335383) collected by Douglas Emlong from the upper Nye Mudstone of Oregon (Emlong field no. E7226).

Revised diagnosis (after Barnes, 1979)—*Pinnarctidion* synapomorphies include w-shaped anterior margin of the nasals, interorbital and postorbital constrictions equal in width, supraorbital process equidistant between the anterior margin of the orbit and the anterior end of the braincase, zygomatic process of squamosal notches the postorbital process of the jugal, widest point of skull across the zygomatic arches lies well anterior of the glenoid fossa, and choanae wide. These apomorphies distinguish *Pinnarctidion* from *Pteronarctos*, *Enaliarctos*, and other stem pinnipeds.

PINNARCTIDION IVERSENI, sp. nov.

Holotype—SDNHM 146624, nearly complete cranium, partial right humerus, cervical vertebra, and fragmentary ribs.

Etymology—The species name honors Terry Iversen, who collected the holotype (in August 2014), along with a wealth of other fossils from coastal Washington State.

Locality—Material described below was recovered on the beach of Merrick's Bay, Clallam County, Washington, at 48°15'30" N, 124°13'45" W (based on the 1:24000 scale Slip Point Quadrangle:USGS, 2014, and information from the collector) from a single siltstone concretion likely transported from the adjacent cliffs. Merrick's Bay lies on the north shore of the Olympic Peninsula, along the Strait of Juan de Fuca. The collection site, SDNHM locality 7283, lies about 2 kilometers southeast of Slip Point, the eastern edge of the

more prominent Clallam Bay. The cliffs bordering Merrick's Bay are mapped as the upper levels of the Pysht Formation and the overlying Clallam Formation (Schasse 2003), but local faults, folds, landslides, and dense vegetation complicate stratigraphic interpretations. The wave-cut platform at Merrick's Bay is littered with resistant concretions as far as 100m from the cliff base. SDNHM locality 7283 is likely equivalent to LACM locality 5561, from which a small, undescribed pinnipedimorph skull, LACM 128004 (Hunt and Barnes, 1994) was recovered; locality UWBM 6133, from which the holotype *Cancer starri*, UWBM 92012 (Berglund and Goedert, 1996), derives; locality USGS 6374, a molluscan fauna locality (Addicott 1976a); and the unnamed locality that produced a tooth fragment of *Kolponomos sp.*, LACM 123547 (Tedford et al., 1994).

Stratigraphy and Age—The lithology of the matrix adhering to SDNHM 146624, and the location from which the fossil-bearing concretion was recovered, suggest that the specimen originates from the uppermost strata of the Pysht Formation or the lowermost levels of the overlying Clallam Formation. The Pysht Formation is the uppermost of three formations making up the Twin River Group (Snavely et al., 1978). The Clallam Formation, the name applied to strata overlying the Pysht Formation between Slip Point and Pillar Point (Addicott, 1976a), is the youngest unit exposed on the Olympic Peninsula's northern shore. At their contact, the gray sandy siltstones and mudstones of the Pysht Formation conformably and gradationally transition to the thick-bedded, tan sandstones of the Clallam Formation. On the modern wave-cut platform at Merrick's Bay, the base of the Clallam Formation is marked by abundant small bivalve fossils and bioturbated sands (pers. comm., J. Goedert, a knowledgeable local fossil collector). SDNHM 146624 was collected ~200 m southeast of this contact, on the surface of what is mapped as the Pysht Formation. The Pysht

Formation is known to produce fossil-bearing calcareous concretions (Nesbitt et al., 2010), similar to the one in which SDNHM 146624 was contained. SDNHM 146624's silty gray mudstone lithology, and its recovery beneath a cliff mapped as the Pysht Formation (Schasse 2003), indicate its likely provenance from that unit.

Biostratigraphic studies place the boundary between the Juanian and Pillarian molluscan stages at the Pysht-Clallam contact (Addicott, 1976b, Nesbitt et al., 2010). Benthic foraminiferal biozonation is less well-defined. The Pysht Formation likely represents the Zemorrian foraminiferal stage while the Clallam Formation may represent the Saucesian (Kleinpell, 1938, Snavely et al., 1978). Nevertheless, taxa limited to the Saucesian in California overlap with Zemorrian taxa in Washington, so a sharp boundary cannot be recognized in this region (Nesbitt et al., 2010). Magnetostratigraphic evidence (Prothero et al., 2001) suggests that the uppermost Pysht Formation correlates with Chron C6Cr and C6Cn3n (23.7-24.7 Ma) and the lower section of the Clallam Formation with Chron C6Cn3n-C6Cn2r (23.8-24.2 Ma), indicating a late Oligocene age for the specimen.

Diagnosis—*Pinnarctidion iverseni* is distinguished from other basal pinnipedimorphs by its accessory cusps on P3 and P4, the strong posterior divergence of its palate, its dorsoventrally deep and dorsally arched zygomatic processes of the jugal, and its prominent preglenoid processes.

Description—The cranium of SDNHM 146624 (Figures 1 and 2) preserves the palate, left zygomatic arch, and basicranium in excellent condition. The left tooth row (Figure 3) consists of a well-preserved set of premolars and M1, along with an anteriorly abraded canine and I3 root. The right maxilla and premolars are abraded labially, revealing the premolar roots in cross-section. The right M1 is preserved, but the canine and incisors are

not. Parts of the skull lost to abrasion by wave action include the anterior tip of the premaxilla, incisors, right zygoma, mastoid and paroccipital processes, occipital condyles, and much of the parietal and occipital portions of the braincase.

SDNHM 146624 represents an adult individual based on its fused proximal humeral epiphysis, anular epiphyses, and cranial sutures, as well as the small wear facets on its teeth. The preserved portion of the cranium of SDNHM 146624 is 142 mm long (the missing incisor row and occipital condyles would have likely contributed less than an additional 20 mm to the skull's length), making it small for an early pinnipedimorph; the skulls of *Pinnarctidion rayi*, *Pteronarctos goedertae*, and *Enaliarctos emlongi* measure 190 mm, 197, and 228 mm, respectively. SDNHM 146624 lacks a sagittal crest, which is unlikely to be an artifact of abrasion, given that the cortical bone is continuous across the smoothly convex sagittal midline. The posterior portion of the skull is too incomplete to indicate whether lambdoidal crests were present. Sagittal and lambdoidal crests occur in *Enaliarctos mealsi* (Mitchell and Tedford 1973), *E. barnesi*, *E. emlongi*, and *E. tedfordi* (Berta 1991); are exaggerated in many specimens of *Pteronarctos goedertae* (Berta 1994b); are reduced in *Pinnarctidion rayi* (Berta 1994a); and are not preserved in *Enaliarctos mitchelli* (Barnes 1979, Berta 1991) or *Pinnarctidion bishopi* (Barnes 1979). The condition of the crests in these taxa has influenced interpretations of sex and ontogeny, the prevailing view being that absent or reduced crests indicate female or immature individuals. SDNHM 146624 likely represents a female, based on its lack of a sagittal crest, slender snout with a posteriorly divergent toothrow, relatively small canine, and small overall size (Berta, 1994b, Sanfelice and de Freitas, 2008, Cullen et al., 2014).

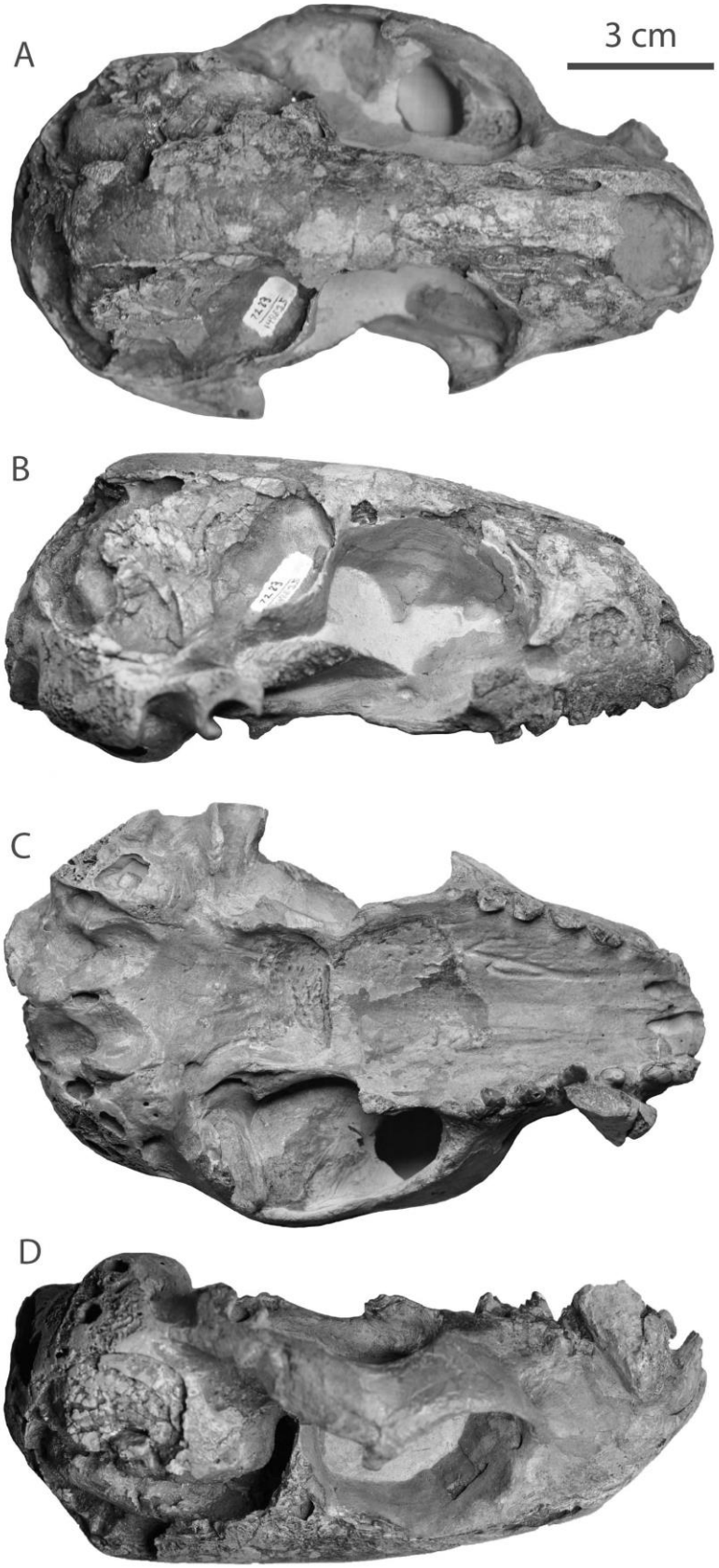
A
3 cm
B
C
D

FIGURE 1. SDNHM 146624 cranium in dorsal (A), right lateral (B), ventral (C), and left lateral (D) views.

Rostrum

The rostrum is tall and narrow compared to the condition in other early pinnipedimorphs. Although the anterior portion of the premaxilla is missing, the rostrum is short for a skull of this size. The narial opening is 27 mm tall and 22 mm wide. The posterior contacts of the nasals are not distinguishable, but the medial suture and the premaxilla contact are visible anteriorly. The nasals are excavated anteriorly; the forward projection of their medial suture results in a w-shaped anterior margin of the two elements.

Orbits

The interorbital region is 23 mm wide at its narrowest point; anteriorly it widens slightly at the supraorbital processes, while posteriorly its width is relatively even. The supraorbital processes of the frontal, which appear slightly abraded, are more posteriorly positioned within the interorbital region than in *Enaliarctos* or *Pteronarctos*. A small but distinct antorbital process occurs on the skull's left side. A 4-mm-wide rounded triangular infraorbital foramen is present. Directly below the antorbital process lies a 2-mm-wide lacrimal foramen, but the sutures of the lacrimal bone are indistinct. The walls of the orbit, largely intact, are deeply set. The width and depth of the orbits indicate that the eyes were large. An opening in the frontal on the right medial orbital wall, posterior to the lacrimal foramen, resembles a perforation described in *Pinnarctidion bishopi*, UCMP 86334 (Barnes, 1979). If these features in UCMP 86334 and SDNHM 146624 are not preservational artifacts, they may be precursors to the orbital vacuity observed in crown pinnipeds. A

concavity posteroventral to the lacrimal foramen likely represents a shallow fossa muscularis. The ventral margin of this concavity meets the dorsal margin of the infraorbital foramen as a low, posteriorly extending ridge, as described in UCMP 86334 (Barnes, 1979). Ventral to this ridge, and anterodorsal to the palatine process, a small posterior palatine foramen perforates the maxilla. The sphenopalatine foramen is obscured by matrix (not removed to reinforce the region).

Zygoma

The left zygomatic arch is well-preserved, but the right is missing. The zygomatic arch bows laterally around the orbital region. A slightly abraded yet still prominent postorbital process projects 4 mm dorsomedially from the center of the arch, following the round contour of the orbit. The ventral surface of the zygomatic arch, flat below the infraorbital foramen, curves strongly dorsally near the jugal-squamosal suture. Posteriorly, the zygomatic arch shallows dorsoventrally as it approaches the base of the braincase. Anteriorly, the zygomatic arch of SDNHM 146624 is deeper than in *E. emlongi* and *E. tedfordi* (Berta, 1991), and turns medially toward the maxilla more abruptly. The zygoma joins the maxilla between M1 and M2. The fused maxillary-jugal suture cannot be discerned. The squamosal process projects anteriorly below the postorbital process of the jugal in a rounded, weakly mortised notch. The overlapping jugal-squamosal suture extends posteriorly to the preglenoid process.

Braincase

The lateral and posterior walls of the braincase are largely weathered and collapsed, but the remaining scaffolding suggests the braincase was transversely broader but posteriorly

shorter relative to those of *Enaliarctos mealsi* or *Pteronarctos goedertae*. The highest point of the cranial roof occurs roughly within the same transverse plane that bisects the posterior lacerate foramina. Though the posterior portion of the skull is heavily abraded, there is no indication that lambdoidal crests were present. The occipital condyles are missing, but the 23-mm-tall and 24-mm-wide opening of the foramen magnum is clearly defined.

Palate

Nearly horizontal anteriorly, the palate becomes more strongly arched posterior of P3. The cheek tooth rows strongly diverge as the palate widens posteriorly. The palate is 23 mm wide between the P1s and 37 mm wide between the M1s. The paired incisive foramina, truncated anteriorly by the abraded edge of the specimen, terminate posteriorly at the level of the P1 root. On either side of the palate, two posteriorly bifurcated palatine sulci occur at the level of P1 and P2, neither of which is continuous with the incisive foramina. Several pores and secondary sulci are also distributed across the palate. The embrasure pits between P4 and M1 are shallow compared to those of *Enaliarctos* species. In contrast to most other arctoids, shallow pits also occur between the premolars of SDNHM 146624. Prominent palatine processes project obliquely from the posterior margin of the palate, extending 15 mm beyond the M2 alveoli. A small sphenopalatine fossa is present at the base of the orbital wall, dorsal to the lateral edge of the maxillary tuberosity. The posterior edge of the palatine process extends a few millimeters posterior to the maxillary tuberosities, forming a broad U-shaped palatal margin with the pterygoids.

Basicranium

Relative to skull size, the pterygoid region of SDNHM 146624 is shorter and broader than in other early pinnipedimorphs; the distance between the left and right pterygoids (26 mm) exceeds the distance from the palatal shelf to the pterygoid hamuli (18 mm). A pointed hamulus projects posteroventrally from each pterygoid process. The lateral pterygoid process extends anterodorsally to a prominent right-angled point, forming a shallow concave fossa between it and the hamulus. The medial pterygoid plate wraps posterolaterally toward the anterior opening of the foramen lacerum. The alisphenoid canal and the foramen ovale share a common fossa beneath the medial pterygoid plate.

The glenoid fossa is deeply excavated and angles slightly anterolaterally. The postglenoid process is most pronounced medially, where it underhangs the glenoid fossa. The preglenoid process is widest toward the lateral margin of the glenoid fossa, as it is in most basal pinnipedimorphs. The preglenoid process of SDNHM 146624 is more pronounced than that of *Pinnarctidion bishopi* (Barnes 1979). A large preglenoid process occurs in *Enaliarctos mealsi* (Mitchell and Tedford 1973) and in some specimens of *Pteronarctos goedertae* (Berta 1994b), but is typically absent or reduced in crown pinnipeds.

The slightly concave basisphenoid bears a slightly uneven medial surface. In the region between the auditory bullae, the basioccipital forms a posteriorly directed v-shaped elevation. From the vertex of this “v”, the clivus extends posteriorly as a ridge along the basioccipital’s midline. The clivus is interrupted by an irregular cavity in the braincase, reminiscent of a similar structure observed in *Phoca vitulina*, but likely an artifact of damage. The basioccipital’s lateral edges bear steep, parentheses-shaped, flanges that curve ventrally and posteromedially at the tympano-occipital fissure. Medial to the posterior lacerate foramina are deep embayments bounded by the raised posterior edges of the basioccipital

flanges. The posterior carotid foramen, posterior lacerate foramen, and hypoglossal foramen are clearly exposed.

Auditory bullae

The auditory bullae (Fig. 2) are moderately expanded ventromedially and abut the basioccipital flange. They become gradually less inflated posterolaterally as they approach the mastoid, and slope abruptly anteriorly toward the pterygoid and squamosal. Abrasion of the surface of the left bulla reveals faint suture lines evidently marking the contact between the ento- and ectotympanics. The ectotympanic is separated from the rostral entotympanic medially along a suture that runs ventral to the carotid canal. The bulla is most expanded medially, peaking just lateral to the rostral entotympanic suture. The bulla does not underlap the basioccipital medially, rather it folds abruptly inward at its contact with the basioccipital flange. This contact diverges widely posteriorly, creating a vi-shaped notch for the large posterior carotid foramen.

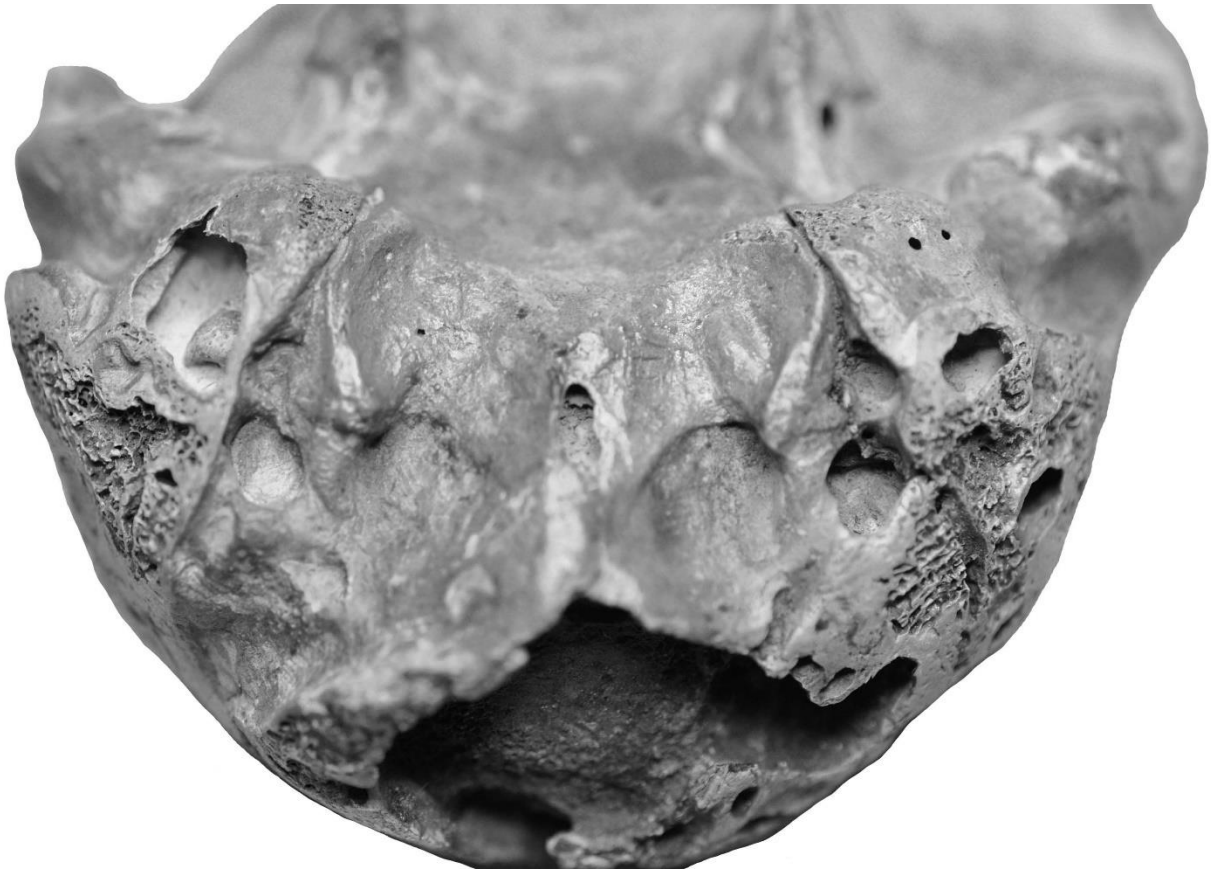

FIGURE 2. Posteroventral view of SDNHM 146624, showing basicranium and auditory bullae.

Upper dentition

The first two upper incisors are not preserved. Of I3, only the posterior end of the root of the left tooth, and the alveolus of the right tooth, remain. Similarly, only a cross-section of the lingual half of the left canine remains, while the alveolus of the right canine tooth is exposed along the narial border. The small preserved portion of the left canine suggests that this tooth was small and slender. The nature of the carinae cannot be determined.

The left premolar series is complete. The teeth are moderately spaced along the toothrow. P1 and P2 are single-cusped, relatively thin, and recurved slightly posteriorly. The

anterior and posterior edges of P1 are convex, uniting posteromedially at a blunt, unworn point. The primary cusp of P2, generally termed the paracone, is crest-like and smooth, except for the sharp posterior carina and its dulled anterior counterpart that extend from the cingulum to the crest. The primary cusps of P2 and P3 are narrower than on P1. The apices of P2 and P3 are worn across an anteromedial plane. The premolars all bear a narrow, crenulated, lingual cingulum.

The crowns of P3 and P4 consist of a large recurved primary cusp analogous to the paracone, a smaller accessory cusp half-way along the posterior edge of the crest, and a small, posterolabial cingular cusp. P3 differs from P4 in having a larger primary cusp and smaller secondary and tertiary accessory cusps. The lingual cingulum of P3 is wide but lacks a protocone or a posterior shelf. Conversely, the lingual cingulum of P4 forms a narrow protocone shelf in the posterolingual corner of the crown. This shelf is highly reduced compared to the condition described in *Enaliarctos mealsi* (Mitchell and Tedford 1973). Small parastyles derived from the terminal crenulation of the lingual cingulum occur on P3-4.

The right premolars are abraded labially to less than half of their original width, providing a clear view of the root cross-sections. P1 is single-rooted whereas P2-4 are double-rooted. The posterior root of P4 is bilobed, the protocone and metacone roots being fused.

The M1, which is double-rooted, is shorter anteroposteriorly and lower dorsoventrally than P4. The crown of M1 tips slightly anteromedially, causing a smaller gap between P4 and M1 than between M1 and M2. M1 is dominated by a low conical paracone and a narrow but elevated metacone. A small protocone forms the posterolingual corner of a low lingual

cingulum, which tapers anteriorly around the base of the paracone. Crenulation on the protocone shelf are finer and subtler than those of the premolars. The corresponding basin is relatively shallow, with a distinct wear pit at its center. Both M2s are represented only by small single-rooted, unbifurcated alveoli.

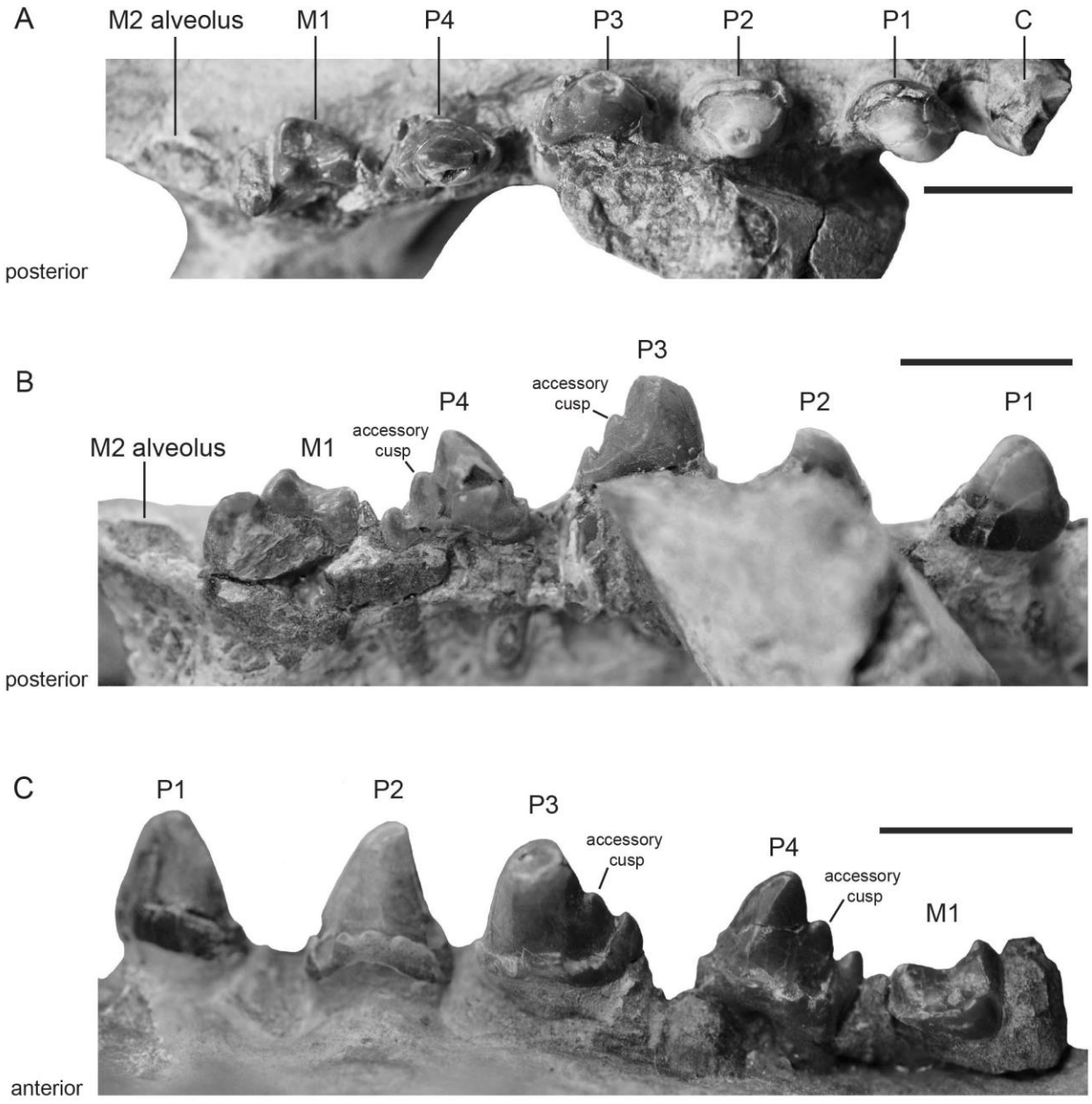

FIGURE 3. SDNHM 146624 upper left tooth row in occlusal (A), labial (B), and lingual (C) views. Scale bar equals 1 cm.

Postcrania

Associated postcranial elements were recovered from the same ~20-cm-long concretion as the skull. The sole preserved vertebra (Figure 4) likely belongs to the cervical series. The right humerus (Figure 5) is also preserved. The distal articular surface and coronoid fossa are not preserved. Associated rib material is too fragmentary for comparative purposes.

Vertebra

SDNHM 146624 preserves a single vertebra (Fig. 4) that rested on the palate along with rib fragments prior to preparation. The vertebra belongs to the cervical series, based on inclination of the centrum, anteroposteriorly broad articular processes, ventrally-projecting transverse processes, and a short spinous process. The inclination of the ventral edge of the transverse processes and moderate height of the spinous process suggest that the element represents C3 or C4.

The centrum is oblique, such that in lateral view the anterior articular surface is higher than the posterior surface, indicating an anterodorsal inclination of the neck. The oval posterior articular surface is interrupted ventrally by a low medial crest that runs most of the length of the centrum but terminates prior to reaching the anterior surface. The anterior articular surface is more elliptical; its dorsal edge is flatter, and its ventral edge is rounder than that of the posterior surface. The vertically projecting spinous process is inclined

slightly anteriorly. The spinous process is abraded dorsally but was likely comparable in length to the zygapophyses. The prezygapophyses, which project anterodorsally and laterally, are even more steeply inclined dorsally (>45°) than the centrum. The postzygapophyses are laterally broad, dorsoventrally flat posterolateral projections of the neural arch lamina. The postzygapophyseal articular surfaces occupy half the ventral length of the projection; they face ventrally and are angled 30° laterally. The transverse processes, broader dorsoventrally than the centrum is high, are angled ventrolaterally. A prominent articular process occurs posteriorly on the end of the left transverse process.

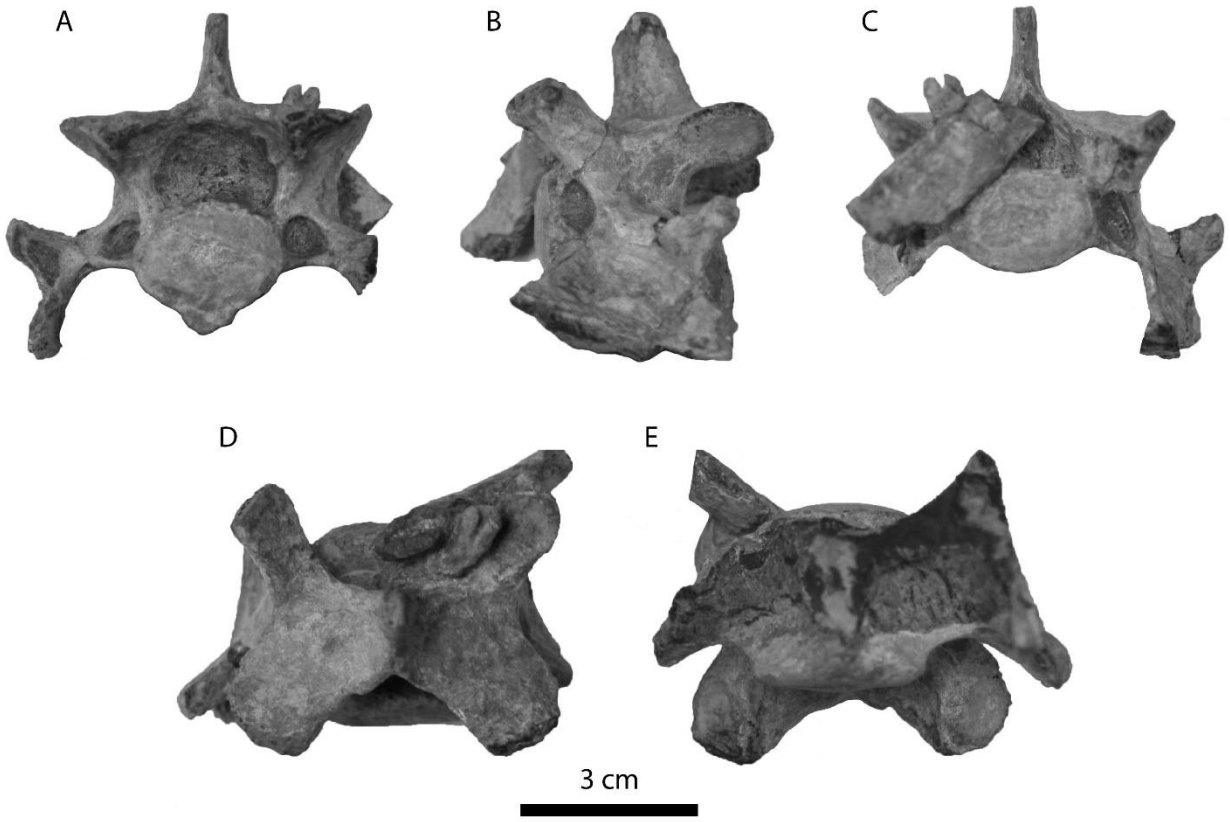

FIGURE 4. SDNHM 146624 cervical vertebra in posterior (A), left lateral (B), anterior (C), dorsal (D), and ventral (E) views.

Humerus

The humerus of SDNHM 146624 is robust and short, as is typical of pinnipedimorphs. The hemispherical head overhangs the diaphysis with a more pronounced curve than in *E. mealsi*. The posterior profile of the diaphysis resembles that of *Pinnarctidion rayi*; it is more concave than in *E. mealsi* or otariids but is less abruptly concave proximally than in phocids. Though both the greater and lesser tuberosities are abraded, neither appears to have been elevated above the head. The long, prominent deltopectoral crest runs roughly two-thirds the length of the shaft. A moderately raised deltoid tuberosity rises along the distal half of the lateral side of the crest. A raised deltoid tuberosity may represent a pinnipedimorph synapomorphy (lutrines and *Puijila* have an elongate deltopectoral crest, but the tubercle does not form a deep fossa or sharp deflection as in pinnipedimorphs). The fossa for the brachialis muscle is shallow. A prominent lateral epicondyle expands posterolaterally from the shaft at about the level that the deltopectoral crest terminates. The distal end of the humerus is lost to abrasion starting from the origin of the medial epicondyle, such that the coronoid fossa and entepicondylar foramen cannot be observed.

FIGURE 5. SDNHM 146624 right humerus in medial (A), posterior (B), lateral (C), and anterior (D) views.

Taxonomic considerations—Although SDNHM 146624 is similar to *Pinnarctidion bishopi* in many respects, it is nonetheless distinctive in several respects. The two most plausible taxonomic assignments for SDNHM 146624 are to refer it (1) to *Pinnarctidion bishopi*, which requires accepting a fair degree of intraspecific variation, or (2) to a new species of *Pinnarctidion* closely related to *P. bishopi*. These alternatives are considered in turn below.

SDNHM 146624 can confidently be assigned to *Pinnarctidion*, based on its large orbits, anteriorly wide zygomatic arches, even thickness across the interorbital constriction, widely spaced cheek teeth, broad pterygoid struts, and wide choanae. SDNHM 146624 shares several important features with the holotype of *Pinnarctidion bishopi* (UCMP 86334), including a dorsoventrally deep zygomatic arch, a notched squamosal-jugal articulation,

presence of lacrimal foramina, posteriorly positioned palatine process of the maxilla, and an M1 paracone lower in relief than the metacone. Phylogenetic analysis indicates that *Pinnarctidion bishopi* is more closely related to SDNHM 146624 than to its congeneric, *P. rayi*, indicating that SDNHM 146624 is nested within the *Pinnarctidion* genus.

SDNHM 146624 differs from the *P. bishopi* holotype in bearing distinct accessory cusps on P3 and P4, a dorsoventrally deeper and more dorsally arched zygomatic process of the jugal, and more exaggerated flanges and embayments of the basioccipital. Since these differences conceivably reflect intraspecific variation or sexual dimorphism, it is necessary to examine how such features vary within better-sampled pinnipedimorph species.

The few basal pinnipedimorphs known from multiple, nearly complete, skulls include *Enaliarctos mitchelli* (Barnes 1979, Berta 1991), *Enaliarctos emlongi* (Berta 1991), *Pinnarctidion rayi* (Berta 1994a), and *Pteronarctos goedertae* (Berta 1994b). The variation observed within each of these taxa can provide a framework for comparing SDNHM 146624 to the *P. bishopi* holotype.

Enaliarctos mitchelli, reported from both the Jewett Sand of California (Barnes 1979) and the Nye Mudstone of Oregon (Berta 1991), may be the only stem pinniped represented by geographically disparate cranial material. The specimen from Oregon (USNM 175637) differs from the holotype from California (UCMP 100391) in its dorsoventrally deeper rostrum, taller narial opening, more dorsally curved zygomatic arch, more elevated postorbital process of the jugal, and in possessing a lacrimal foramen, additional posterior palatal foramina, and rounded rather than pointed palatine processes of the maxilla. Neither specimen from California preserves cheek teeth or posterior portions of the skull, hindering further comparison with USNM 175637. The apparent differences and missing features raise

the question whether USNM 175637 represents a regional variant of *E. mitchelli* or a distinct taxon. In the case of *E. mitchelli*, there is not enough information to confidently interpret variability within this taxon.

Enaliarctos emlongi is known from three skulls (USNM 250345, 314540, and 314290) from the Nye Mudstone of Oregon. USNM 314290, considerably smaller than the others, possibly represents an immature individual (Berta 1991). Subsequent analyses suggested that it may instead be an adult female, based on the pattern of suture closure and the dimorphic female characteristics such as a narrower rostrum and a reduced sagittal crest (Cullen et al. 2014). The dentitions of all three specimens are very similar and lack accessory cusps on the premolars.

Pinnarctidion rayi is known from three specimens (USNM 314325, 250321, and 335383) from the Nye Mudstone of Oregon. The depressions in the basioccipital of USNM 250321, interpreted as a young adult, are less pronounced than those of the holotype (Berta 1994a). The teeth of the three specimens differ only in the size of the protocones. The paracones are all fairly simple and lack accessory cusps.

Pteronarctos goedertae, the best-sampled early pinnipedimorph species, is known from at least 11 skulls from the Astoria Formation of Oregon. These skulls exhibit minor differences in the curvature of the zygomatic arch, but do not capture the large differences in depth and dorsal arching seen between SDNHM 146624 and the holotype of *Pinnarctidion bishopi*. *P. goedertae* specimens differ mainly in the size of the sagittal crests and the relative breadth of the rostrum, both of which are ascribed to sexual dimorphism (Berta 1994b). Despite the limited number of cheek teeth known for P. goedertae, clear evidence of accessory cusps on the paracone or metacone crests is lacking.

Extant pinnipeds provide an opportunity to examine the range of intraspecific morphological variability. For example, *Callorhinus ursinus* varies widely in several continuous cranial characters such as the length of the ascending process of the premaxilla or the length of the pterygoid process (Berta 1994b). Linear measurements may adequately describe variation in more conservative aspects of morphology, but complex shapes such as the zygomatic arch or the tooth cusps require different methods. Though useful for comparing individuals with the same discrete characters, these results do not offer clear guidance for assessing differences in tooth cusps or features with complex shapes like the zygomatic arch. Extant pinniped species tend only to vary in number of cheek teeth or position of the teeth on the palate. The cusps themselves are thought to be highly conserved within species (Drehmer et al. 2015).

Judging from the features known to vary in modern and ancient pinnipedimorphs, the differences between SDNHM 146624 and the holotype of *Pinnarctidion bishopi* are perhaps best interpreted as indicating that these specimens represent different species. The zygomatic arch of SDNHM 146624 is deeper dorsoventrally and more dorsally arched than would be expected in a variant of *P. bishopi*. The flanges and embayments of the basioccipital do not appear to vary within pinnipedimorph species; rather, this region has been used to consider the relations of pinnipedimorphs to other arctoids (Hunt and Barnes 1994). The accessory cusps on the upper postcanines of SDNHM 146624 are highly unusual among basal pinnipedimorphs and provide perhaps the most secure basis for assigning this specimen to a new species.

Though the systematic placement of SDNHM 146624 ultimately hinges on morphology, the geographic and temporal implications may also be considered. If SDNHM

146624 is referred to *Pinnarctidion bishopi*, this species would have ranged from California to Washington. Most basal pinnipedimorphs are known only from a single specimen or from a single stratigraphic unit, so we know little about their geographic ranges. The few exceptions offer limited information. A mandible referable to *Enaliarctos mealsi* has been reported from Schooner Gulch, California (Poust and Boessenecker 2018), extending its known range northward from the type locality in the Jewett Sand Formation (Mitchell and Tedford, 1973). *Enaliarctos mitchelli* is also represented by cranial material from both California and Oregon, though as discussed earlier, there is potential uncertainty about the referral of the Oregon specimen. To use a well-studied modern example, the extant *Callorhinus ursinus* ranges from ~60°N in the Bering Sea to ~34°N in California (Kenyon and Wilke 1953). Assuming the ranges of early pinnipedimorphs mirrored those of modern species, the 12° of latitude separating SDNHM 146624 and UCMP 86334 would not seem unreasonable. However, the current sampling of early pinnipedimorph fossils does not permit proper assessment of their geographic ranges.

The potential overlap in the ages of SDNHM 146624 and UCMP 86334 allows room for speculation that the two could have been contemporaneous. The uppermost beds of the Pysht Formation, which likely produced SDNHM 146624, have been dated to 23.7-24.7 Ma based on magnetic stratigraphy (Prothero et al., 2001). This correlates well with the 25-24 Ma age reported for the Pyramid Hill Sand Member of the Jewett Sand, based on strontium isotope analyses of pecten shells, biostratigraphy, and stratigraphic correlation (Hosford-Scheirer and Magoon 2007). Yet the possibility of temporal overlap should not influence our interpretations of the evolutionary relationship of these morphologically distinct fossils.

Despite the similarities between SDNHM 146624 and the holotype of *Pinnarctidion bishopi*, their differences, particularly the presence of P3 and P4 accessory cusps, are not consistent with the variation observed within other pinnipedimorph species. Therefore SDNHM 146624 is assigned to a new species, *Pinnarctidion iverseni*.

II. Phylogenetic Analysis of Pinnipedimorpha

Methods

The relationships of SDNHM 146624 and other early pinnipedimorphs were investigated through phylogenetic analysis. The character-taxon matrix supporting this analysis consisted of 103 craniodental characters, compiled from the literature (Berta 1991, Berta and Wyss 1994, Deméré and Berta 2002, Boessenecker and Churchill 2018) and original observations. Character states were scored based on firsthand examinations of holotype specimens at LACM, MVZ, and UCMP, as well as from published descriptions and photographs. The matrix was developed in Excel and Notepad.

Thirty caniform taxa were sampled. *Canis lupus* was selected as the outgroup based on strong evidence for the early divergence of canids from the other major caniform clades (Wyss and Flynn 1993, Flynn et al. 2005, Nyakatura and Bininda-Emonds 2012). *Ursus arctos* and *Kolponomos clallamensis* served as representative ursoids, *Neovison vison, Lontra canadensis,* and *Enhydra lutris* as mustelids. Extant pinnipeds were represented by *Phoca vitulina, Erignathus barbatus, Monachus monachus, Odobenus rosmarus, Callorhinus ursinus* and *Zalophus californianus.* Fossil pinnipedimorphs included *Enaliarctos mealsi, E. barnesi, E. emlongi, E. tedfordi, E. mitchelli, Pteronarctos goedertae, Pinnarctidion bishopi*,

Pinnarctidion rayi, Devinophoca claytoni, Thalassoleon mexicanus, Proneotherium repenningi, Imagotaria downsi, Gomphotaria pugnax, Allodesmus kernensis, and *Desmatophoca oregonensis*. *Pteronarctos piersoni* (Barnes 1990) and *Pacificotaria hadromma* (Barnes 1992) were treated as synonyms of *Pteronarctos goedertae* (sensu Berta 1994b). The affinities of the enigmatic amphibious arctoids *Potamotherium valletoni* and *Puijila darwini* were also tested herein. Because the characters used in this study were selected specifically to investigate evolutionary relationships within Pinnipedimorpha, we attach little significance to the branching sequence of other carnivoran clades specified by our analyses.

A heuristic parsimony analysis was conducted in TNT (Tree analysis using New Technology) version 1.5 (Goloboff et al., 2003), using a traditional search of Wagner trees and tree bisection and reconnection (TBR) branch swapping with 1000 random addition sequences and 10 trees retained per round. No weighting or ordering was imposed on any of the characters. Bremer support values, or the number of additional steps needed to unresolve a given clade, were calculated for the strict consensus maximum parsimony tree. Data were also subjected to bootstrap and jackknife resampling analyses to further assess branch support.

Results

Parsimony analysis produced two most parsimonious trees, both 526 steps in length (see Fig. 6), differing only in the placement of *Pteronarctos* and *Pinnarctidion*. Clades recovered from parsimony analysis will be discussed in order of divergence from the base of the tree.

Ursidae plus Mustelidae were recovered to form the sister clade to Pinnipedimorpha. This relationship is inconsistent with most recent studies (Fulton and Strobeck 2006, Nyakatura and Bininda-Emonds 2012, Luan et al. 2013), which identify either ursids or mustelids as closer to pinnipeds. The few studies to consider an ursid plus mustelid clade recovered this topology with weak support, based on combined molecular and morphologic data (Flynn and Nedbal 1998) or mitochondrial genes (Delisle and Strobeck 2005). Poor resolution at the base of the arctoid tree suggests that a different set of characters and a more diverse set of fossil and recent taxa need to be considered to appropriately test those relationships.

Potamotherium valletoni and *Puijila darwini* are recovered as the earliest diverging members of Pinnipedimorpha, respectively, primarily on the basis of shared features of the auditory region (see Appendix 4). This is consistent with other studies of the recently discovered *Puijila* (Rybczynski et al., 2009, Paterson et al., 2020). *Potamotherium*, known from abundant material, has a checkered taxonomic history, having been interpreted as a lutrine mustelid (Savage 1957), semantorid phocid (Tedford 1976), semantorid mustelid (de Muizon 1982a), stem mustelid (Schmidt-Kittler 1981), or oligobunine mustelid (Wang et al. 2005). Clearly more detailed investigation of these curious taxa is warranted.

The five recognized species of *Enaliarctos* were recovered as highly paraphyletic, contradicting previous consideration of their relationships (Berta 1991). Berta's study used 16 morphological characters to compare the five *Enaliarctos* species to a generalized ursid outgroup, reporting a monophyletic Enaliarctos clade, yet conceding that monophyly "cannot be unambiguously determined". Nevertheless, the strict monophyletic interpretation of that study continues to be reported in the review literature (Poust and Boessenecker 2018, Berta

et al. 2018). A recent study of pinnipedimorph phylogeny found *Enaliarctos* to be paraphyletic (Paterson et al. 2020), but with a different topology from the one advocated here. The results of the current study indicate morphological trends within the '*Enaliarctos*' grade, including a reduction of M1, an increase in orbit size, a series of shifts in the position of the zygomatic arch. It is important that we acknowledge *Enaliarctos* as a paraphyletic grade of successively branching lineages in order to recognize trends in early pinnipedimorph evolution that may be ignored if one assumes *Enaliarctos* monophyly.

The relationships between *Pteronarctos*, *Pinnarctidion*, and *Proneotherium* plus Pinnipedia remain unresolved, these taxa forming the only polytomy in the strict consensus tree. This result supports the recent notion that *Pinnarctidion* lies outside of crown Pinnipedia (Boessenecker and Churchill 2018), as opposed to initial claims that it was closer to allodesmines (Barnes 1979) or phocids (Berta 1994a, Berta & Wyss 1994). Despite the polytomy, several character transformations occur in this part of the tree. The clearest trends are toward reduction of the carnassial region of the toothrow relative to terrestrial carnivorans and earlier-diverging pinnipedimorphs. Associated traits include reduction of the P4 protocone shelf, a double-rooted P4, and shallowing of the embrasure pits between P4 and M1. The posterior portion of the palate broadens at this node of the tree, and the palatine processes expand to form a more prominent shelf.

Proneotherium, generally considered an early odobenid that retained primitive characters (Deméré and Berta 2001, Boessenecker and Churchill 2013), is resolved outside of crown Pinnipedia. Its exclusion from the crown clade reflects the retention of several primitive dental features such as an I3 lingual cingulum, a double-rooted M1, an M1 protocone shelf, and a shallow embrasure pit between P4 and M1. One alternative but less

parsimonious explanation is that early odobenids (including *Proneotherium*) acquired distinctive postcranial features before convergently losing various primitive dental features. The alternative suggested here is that *Proneotherium* diverged prior to the origin of Pinnipedia, and its postcranial resemblances to odobenids are convergent.

Pinnipedia is composed of an otariid clade and an odobenid plus phocoid clade. The crown group is supported by synapomorphies related to a simplified dentition, such as a single-rooted M1 with no protocone shelf, no I3 lingual cingulum, and no embrasure pit between P4 and M1. The otariid clade places *Thalassoleon* sister to *Zalophus* plus *Callorhinus*. Features diagnosing this group include the frontal bone intruding between the nasals, a prominent supraorbital process, and narrow, cuspate premolar cingula. The odobenid-phocoid clade consists of *Gomphotaria* plus *Odobenus* and (*Imagotaria* (*Allodesmus* (*Desmatophoca* (*Devinophoca* (*Monachus* (*Erignathus* plus *Phoca*)))))). Synapomorphies of this clade involve the auditory region, including the petrosal visible through the posterior lacerate foramen, enlarged auditory ossicles, and the canal for the cochlear aqueduct merged with the round window. These results are largely compatible with previous morphological phylogenies (Berta and Wyss 1994, Berta et al. 2018), although the placement of certain taxa within the crown clade, such as *Imagotaria*, *Allodesmus*, and *Desmatophoca*, contradicts recent work (Boessenecker and Churchill 2013, 2018; Velez-Juarbe 2017). The consistent morphological evidence for uniting odobenids and phocids contrasts with molecular studies favoring an otarioid (odobenid plus otariid) clade (Flynn and Nedbal 1998, Fulton and Strobeck 2006, Nyakatura and Bininda-Emonds 2012). Relationships within crown Pinnipedia require further testing, albeit with a set of characters better calibrated for within-crown comparisons than that used in this study.

Bremer support values for nodes on the strict consensus trees (Figure 7) vary between 1 and 10. The most robustly supported clades recovered in the analysis are *Lontra* plus other mustelids, *Enaliarctos tedfordi* plus other pinnipedimorphs, and *Erignathus* plus *Phoca.*

Resampling analyses recovered topologies different from those of the maximum parsimony trees. Bootstrap analyses, in which trees are generated from a random sampling of characters, are highly variable and do not provide a direct measure of confidence (Siddall, 2002). However, observed bootstrap proportions of 70 or greater have been found to correspond with a 95% confidence index (Hillis and Bull, 1993). Therefore, the most strongly supported clades as judged by bootstrap resampling (Figure 8) are *Lontra* plus other mustelids, *Enaliarctos tedfordi* plus other pinnipedimorphs, *Pinnarctidion iverseni* plus *Pinnarctidion bishopi*, *Gomphotaria* plus *Odobenus*, *Devinophoca* plus other phocids, and *Erignathus* plus *Phoca*.

Jackknifing, which analyzes subsets of characters from a given matrix, measures the effects of character sampling and variance in a dataset but does not provide a direct measure of branch support (Siddall, 2002). The tree produced through jackknifing (Fig. 9) is nearly identical to maximum parsimony Tree 1 (Fig. 6), apart from the pairing of *Desmatophoca* and *Allodesmus* in the former. This similarity of maximum parsimony and jackknifing results suggests that character sampling had little influence on the topology of the tree favored in this study.

In the maximum parsimony and the resampled trees, the paring of *Pinnarctidion iverseni* and *Pinnarctidion bishopi* is supported by six synapomorphies: presence of a lacrimal foramen, multiple palatine foramina, an oblique palatine process, inflation of the auditory bullae limited to the ectotympanic, a reduced P4 metacone, and M1 metacone more

prominent than paracone. Apomorphies of *Pinnarctidion iverseni* distinguishing it from *P. bishopi* include a dorsoventrally deeper zygomatic arch, more divergent palate, more arched palate, more laterally prominent preglenoid process, round foramen magnum, accessory cusp on P3 and P4, and a simple (unlobed) M1 posterior root.

Each additional species of early pinnipedimorph helps to resolve the sequence of character transformations that occurred during this lineage's transition from a terrestrial to an aquatic environment. Pinnipeds are known for their flipper-like limbs, which we know were acquired before the appearance of *Enaliarctos mealsi* (Berta et al. 1989). The skull and teeth, however, record changes in morphology that were at least partly decoupled from the evolution of the limbs. The most evident and perhaps the most functional of these changes involve the dentition. A shift away from the large carnassial cheek teeth of terrestrial carnivorans, toward the more conical teeth of typical aquatic predators, is clearly documented in the pinniped stem. A reduced P4 and highly reduced M1 and M2 is present in the earliest species of *Enaliarctos*. Reduction and posterior placement of the P4 protocone is present in the later-diverging *Pteronarctos* and *Pinnarctidion*. The embrasure pit between P4 and M1 is reduced and subsequently lost, and the P4 metacone and paracone is reduced until it is of comparable size to the rest of the cheek teeth. These changes occurred after the acquisition of flippered limbs, but prior to the origin of crown Pinnipedia, during a period of pinnipedimorph radiation into aquatic habitats of the late Oligocene and early Miocene.

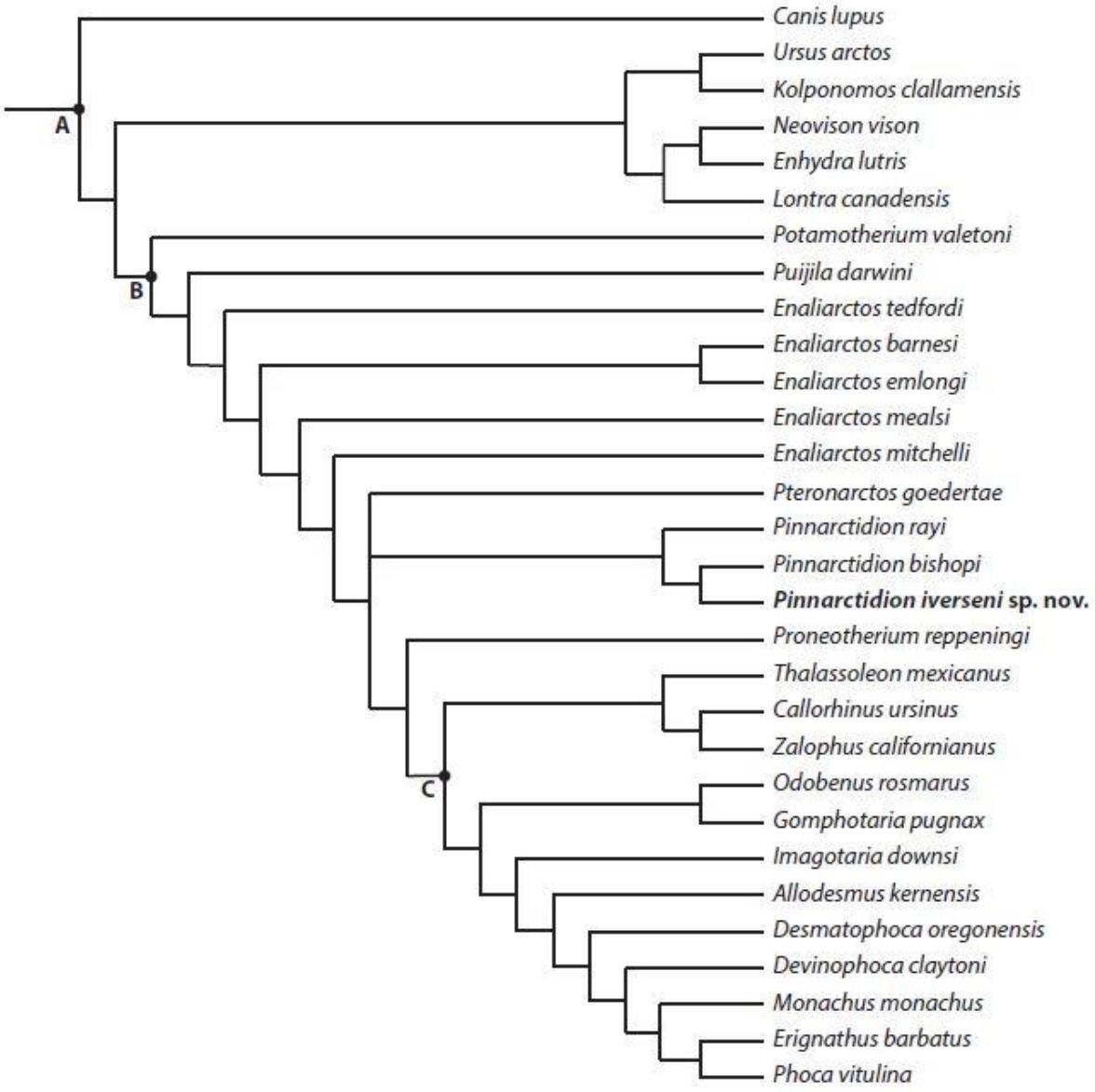
A
B
C
Canis lupus
Ursus arctos
Kolponomos clallamensis
Neovison vison
Enhydra lutris
Lontra canadensis
Potamotherium valetoni
Puijila darwini
Enaliarctos tedfordi
Enaliarctos barnesi
Enaliarctos emlongi
Enaliarctos mealsi
Enaliarctos mitchelli
Pteronarctos goedertae
Pinnarctidion rayi
Pinnarctidion bishopi
Pinnarctidion iverseni sp. nov.
Proneotherium reppeningi
Thalassoleon mexicanus
Callorhinus ursinus
Zalophus californianus
Odobenus rosmarus
Gomphotaria pugnax
Imagotaria downsi
Allodesmus kernensis
Desmatophoca oregonensis
Devinophoca claytoni
Monachus monachus
Erignathus barbatus
Phoca vitulina

FIGURE 6. Strict consensus tree of the two maximally parsimonious trees based on 103 craniodental characters. “A” represents Caniformia, “B” represents Pinnipedimorpha, and “C” represents Pinnipedia. See Appendix 4 for list of synapomorphies associated with each clade.

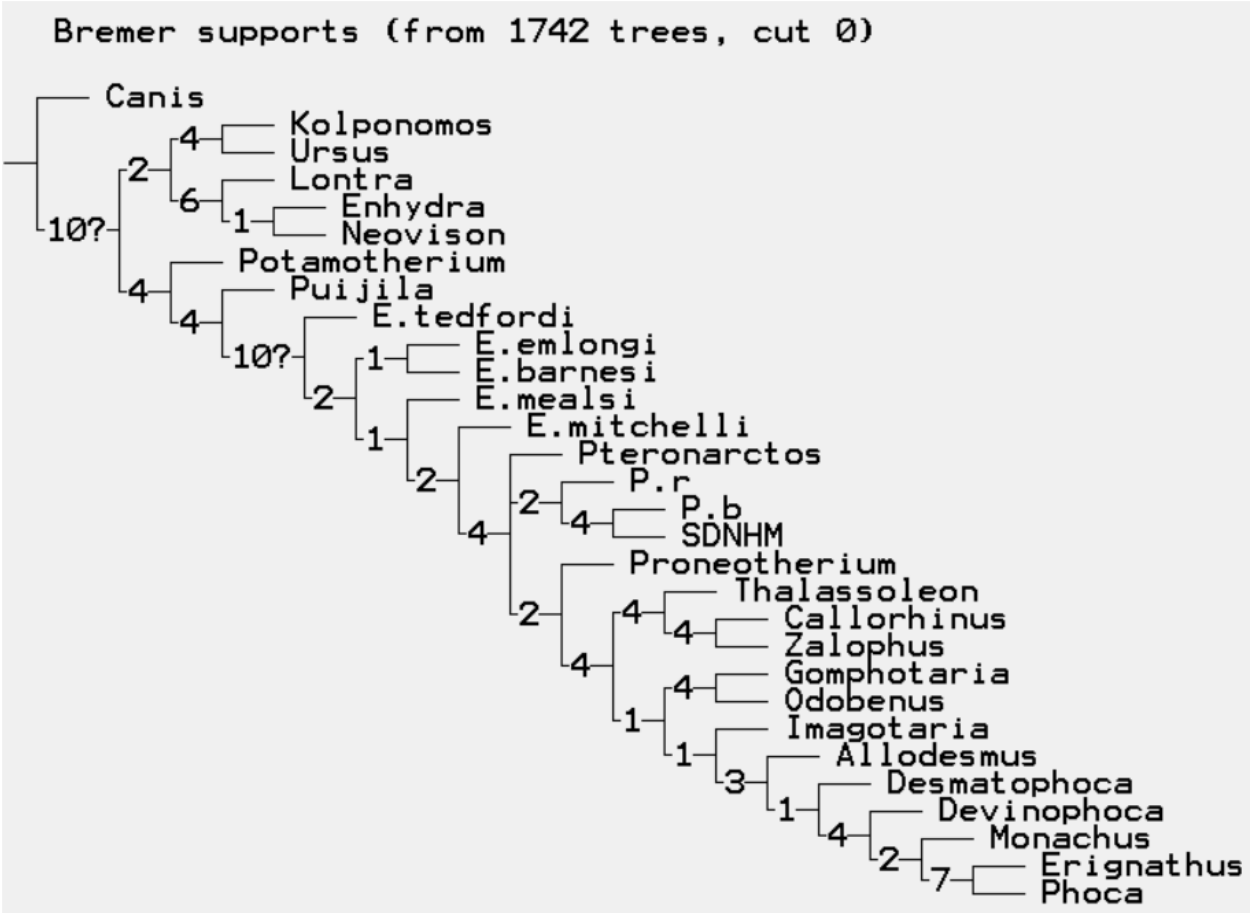

FIGURE 7. Bremer support values for the strict consensus of the two most parsimonious trees. Numbers represent the additional steps needed to unresolve a given clade.

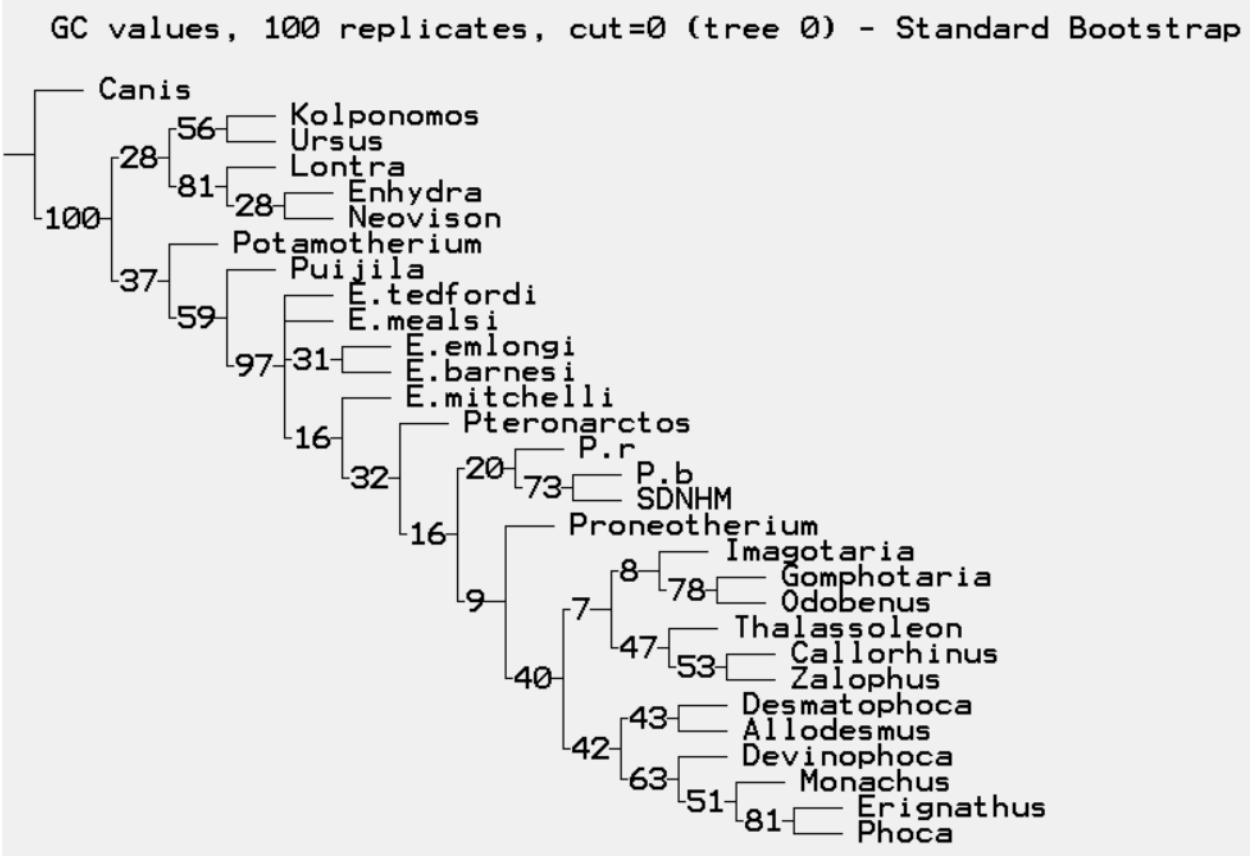

FIGURE 8. Standard bootstrap resampling. Support values represent the frequency of nodal support given 100 replicates.

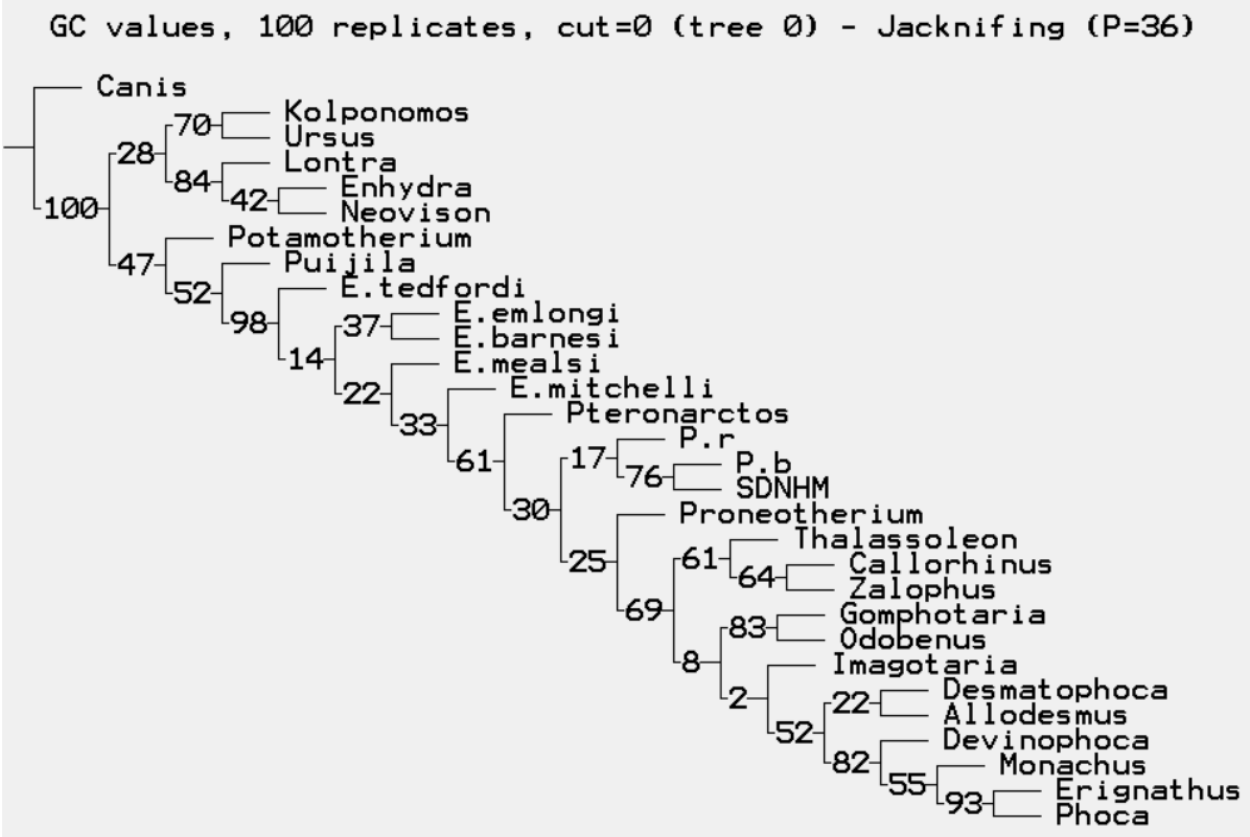

FIGURE 9. Standard jackknife resampling. Support values represent the frequency of nodal support given 100 replicates.

References

Adam, P.J., and Berta, A. 2001. Evolution of prey capture strategies and diet in Pinnipedimorpha (Mammalia, Carnivora). *Oryctos*, 4: 3-27.

Addicott, W.O. 1976a. Molluscan paleontology of the lower Miocene Clallam Formation, western Washington. U.S. Geological Survey Professional Paper, 976, 1-44.

Addicott, W.O., 1976b. Neogene molluscan stages of Oregon and Washington. In: The Neogene Symposium, selected papers on paleontology, sedimentology, petrology, tectonics and geologic history of the Pacific Coast of North America. Pacific Section SEPM, Los Angeles, California, 95–115.

Arnason, U., Gullberg, A., Janke, A., Kullberg, M., Lehman, N., Petrov, E.A., and Väinölä, R. 2006. Pinniped phylogeny and a new hypothesis for their origin and dispersal. *Mol. Phylogenet. Evol.* 41, 345–354.

Barnes, L.G. 1972. Miocene Desmatophocinae (Mammalia: Carnivora) from California. *Univ. Calif. Publ. Geol. Sci.*, 89:1-68.

Barnes, L.G. 1979. Fossil Enaliarctine Pinnipeds (Mammalia: Otariidae) from Pyramid Hill, Kern County, California. *Contributions in Science, Natural History Museum of Los Angeles County*, 318:1-41.

Barnes, L.G. 1989. A New Enaliarctine Pinniped from the Astoria Formation, Oregon, and a Classification of the Otariidae (Mammalia: Carnivora). *Contributions in Science, Natural History Museum of Los Angeles County*, 403:1-26.

Barnes, L.G. 1990. A new Miocene Enaliarctine Pinniped of the Genus *Pteronarctos* (Mammalia: Otariidae) from the Astoria Formation, Oregon. Contrib. Sci. 422, Mus. Nat. Hist. Los Angeles Cty., Los Angeles, CA

Barnes, L.G. 1992. A new genus and species of middle Miocene enaliarctine pinniped (Mammalia: Carnivora) from the Astoria Formation in Coastal Oregon. Contrib. Sci. 431, Mus. Nat. Hist. Los Angeles Cty., Los Angeles, CA

Barnes, L.G. and Raschke, R.E. 1991. *Gomphotaria pugnax*, a new genus and species of late Miocene dusignathine otariid pinniped (Mammalia: Carnivora) from California. *Contributions in Science* 426:1-16.

R. E. Berglund and J. L. Goedert. 1996. A new crab (Brachyura: Cancridae) from lower Miocene rocks of the Northwestern Olympic Peninsula, Washington. *Journal of Paleontology* 70(5): 830-835.

Berta, A. 1991. New *Enaliarctos* (Pinnipedimorpha) from the Oligocene and Miocene of Oregon and the role of "Enaliarctids" in pinniped phylogeny. *Smithsonian Contributions to Paleobiology* 69:1–36.

Berta A. 1994a. A new species of phocoid pinniped *Pinnarctidion* from the early Miocene of Oregon. *J. Vertebr. Paleontol.* 14:405–13

Berta A. 1994b. New Specimens of the Pinnipediform *Pteronarctos* from the Miocene of Oregon. *Smithson. Contrib. Paleobiol.* 78. Washington, DC: Smithson. Inst. Press

Berta, A., Ray, C.E., and Wyss, A.R. 1989. Skeleton of the Oldest Known Pinniped, *Enaliarctos mealsi*. *Science* 244:60–62.

Berta, A., and Wyss, A.R. 1994. Pinniped Phylogeny. In: Contributions in marine mammal paleontology honoring Frank C. Whitmore, Jr. *Proceedings of the San Diego Society of Natural History* 29:33-56.

Berta, A., Churchill, M., and Boessenecker, R. 2018. The Origin and Evolutionary Biology of Pinnipeds: Seals, Sea Lions, and Walruses. *Annual Review of Earth and Planetary Sciences* 46:203-28.

Boessenecker, R.W., Churchill, M. 2013. A reevaluation of the morphology, paleoecology, and phylogenetic relationships of the enigmatic walrus Pelagiarctos. PLOS ONE 8:e54311

Boessenecker, R.W. and Churchill, M. 2018. The last of the desmatophocid seals: a new species of *Allodesmus* from the upper Miocene of Washington, USA, and a revision of the taxonomy of Desmatophocidae. *Zoological Journal of the Linnean Society,* 184(1).

Bowditch, T.E. 1821. An Analysis of the Natural Classifications of Mammalia for the Use of Students and Travelers. J. Smith, Paris.

Condon, T. 1906. A new fossil pinniped (*Desmatophoca oregonensis*) from the Miocene of the Oregon coast. University of Oregon Bulletin 3(3):1-14.

Cullen, T.M., Fraser, D., Rybczynski, N., Schroder-Adams, C. 2014. Early evolution of sexual dimorphism and polygyny in Pinnipedia. Evolution 68:1469–84.

Delisle, I. and Strobeck, C. 2005. A phylogeny of the Caniformia (order Carnivora) based on 12 complete protein-coding mitochondrial genes. Mol. Phylogenet. Evol. 37: 192-201

Deméré, T., and Berta, A. 2001. A reevaluation of *Proneotherium repenningi* from the Miocene Astoria Formation of Oregon and its position as a basal odobenid (Pinnipedia: Mammalia). Journal of Vertebrate Paleontology 21:270–310.

Deméré, T.A., Berta A., Adams P. 2003. Pinnipedimorph evolutionary biogeography. *Bull. Am. Mus. Nat. Hist.* 13:32–76.

de Muizon, C. 1982a. Les relations phylogénétiques des Lutrinae (Mustelidae, mammalia) Geobios Mem. Spec. 6, 259–277.

de Muizon, C. 1982b. Phocid phylogeny and dispersal. *Ann. S. Afr. Mus.* 89:175–213.

Flower, W.H. 1869. On the value of the characters of the base of the cranium in the classification of the Order Carnivora and the systematic position of Bassaris and other disputed forms. Proc. Zool. Soc. London, 1869: 4-37.

de Queiroz, K. and Gauthier, J. 1990. Phylogeny as a Central Principle in Taxonomy: Phylogenetic Definitions of Taxon Names. Systematic Biology 39(4): 307-322.

Drehmer, C. J., Sanfelice, D., and Loch, C. 2015. Dental anomalies in pinnipeds (Carnivora: Otariidae and Phocidae): occurrence and evolutionary implications. Zoomorphology. 134:325-338.

Flynn, J.J. and Nedbal, M.A. 1998. Phylogeny of the Carnivora (Mammalia): congruence vs incompatibility among multiple datasets. Mol. Phylogenet. Evol. 9: 414-426.

Flynn, J.J., Finarelli, J.A., Zehr, S., Hsu, J., Nedbal, M.A. 2005. Molecular Phylogeny of the Carnivora (Mammalia): Assessing the Impact of Increased Sampling on Resolving Enigmatic Relationships, *Systematic Biology* 54(2):317–337.

Fulton, T.L., Strobeck, C. 2006. Molecular phylogeny of the Arctoidea (Carnivora): effect of missing data on supertree and supermatrix analyses of multiple gene data sets. Mol. Phylogenet. Evol. 41:165–81.

Goloboff, P., Farris, J., Nixon, K. 2003. T.N.T.: Tree Analysis Using New Technology. Program and documentation, available at http://www.zmuc.dk/public/phylogeny/tnt.

Higdon, J.W., Bininda-Emonds, O.R.P., Beck, R.M.D., Ferguson, S.H. 2007. Phylogeny and divergence of the pinnipeds (Carnivora: Mammalia) assessed using a multigene dataset. *BMC Evol. Biol.* 7(216).

Hillis, D.M., Bull, J.J. 1993. An empirical test of bootstrapping as a method for assessing confidence in phylogenetic analysis. *Syst. Biol.* 42-182-192.

Hosford-Scheirer, A. and L.B. Magoon 2007. Age, distribution, and stratigraphic relationship of rock units in the San Joaquin Basin province, California. US Geological Survey Professional Paper 1713:1–107.

Hunt, R.M. and Barnes, L.G. 1994. Basicranial evidence for ursid affinity of the oldest pinnipeds. In: Contributions in marine mammal paleontology honoring Frank C. Whitmore, Jr. *Proceedings of the San Diego Society of Natural History* 29:57–67.

Huxley, T.H. 1880. On the application of the laws of evolution to the arrangement of the Vertebrata, and more particularly of the Mammalia. Proc. Royal Soc. London, 43: 649-662.

Kenyon, K.W. and Wilke, F. 1953. Migration of the northern fur seal, *Callorhinus ursinus*. Journal of Mammalogy 34: 86–98.

Kleinpell, R.M. 1938. Miocene stratigraphy of California. American Association of Petroleum Geologists, Tulsa, Oklahoma.

Kohno, N., Barnes, L. G., and Hirota, K. 1995. Miocene fossil pinnipeds of the genera *Prototaria* and *Neotherium* (Carnivora; Otariidae; Imagotariinae) in the North Pacific Ocean: Evolution, relationships and distribution. *The Island Arc* 3:285-308

Koretsky, I.A. and Holec, P. 2002. A primitive seal (Mammalia: Phocidae) from the Early Middle Miocene of Central Paratethys. *Smithsonian Contributions to Paleobiology*, 93: 163-178.

Koretsky, I.A., Barnes, L.G., and Rahmat, S.J. 2016. Re-evaluation of morphological characters questions current views of pinniped origins. *Vestik zoologii,* 50(4): 327-354.

Luan P.T., Ryder O.A., Davis H., Zhang Y.P., and Yu, L. 2013. Incorporating indels as phylogenetic characters: impact for interfamilial relationships within Arctoidea (Mammalia: Carnivora). *Mol. Phylogenet. Evol*. 66:748–56.

Mitchell, E.D. 1966. The Miocene pinniped *Allodesmus*. *University of California Publications in Geological Sciences* 61:1-105.

Mitchell, E.D. 1968. The Mio-Pliocene pinniped *Imagotaria*. *Journal of the Fisheries Research Board of Canada* 25(9):1843-1900.

Mitchell, E.D. and Tedford, R.H. 1973. The Enaliarctinae: a new group of extinct aquatic Carnivora and a consideration of the origin of the Otariidae. *Bulletin of the American Museum of Natural History* 151:201–284.

Miyazaki S., Horikawa H., Kohno N., Hirota K., Kimura M., et al. 1994. Summary of the fossil record of pinnipeds of Japan, and comparisons with that from the eastern North Pacific. *Island Arc* 3:361–72.

Nesbitt, E.A., Martin, R.A., Carroll, N.P., and Grieff, J. 2010. Reassessment of the Zemorrian foraminiferal Stage and Juanian molluscan Stage north of the Olympic Mountains, Washington State and Vancouver Island. *Newsletter on Stratigraphy*, 43, 275-291.

Nyakatura, K., Bininda-Emonds, O.R.P. 2012. Updating the evolutionary history of Carnivora (Mammalia): a new species-level supertree complete with divergence time estimates. BMC Biol. 10:12.

Paterson, RS, Rybczynski, N, Kohno, N and Maddin, HC. 2020. A Total Evidence Phylogenetic Analysis of Pinniped Phylogeny and the Possibility of Parallel Evolution Within a Monophyletic Framework. Front. Ecol. Evol. 7:457.

Poust, A.W. and Boessenecker, R.W. 2018. Expanding the geographic and geochronologic range of early pinnipeds: New specimens of Enaliarctos from Northern California and Oregon. Acta Palaeontologica Polonica 63 (1): 25–40.

Prothero, D.R., Streig, A. and Burns, C. 2001. Magnetic stratigraphy and tectonic rotation of the upper Oligocene Pysht Formation, Clallam County, Washington. 224–233. In Prothero, D.R. (ed.) *Magnetic stratigraphy of the Pacific Coast*. The Pacific Section SEPM, Sante Fe Springs, CA.

Repenning C.A., Tedford R.H. 1977. Otarioid seals of the Neogene. Prof. Pap. 992, US Geol. Surv., Washington, DC

Repenning C.A., Ray C.E., Grigorescu D. 1979. Pinniped biogeography. In Historical Biogeography, Plate Tectonics, and the Changing Environment, ed. J. Gray, A.J. Boucot, pp. 357–69. Corvallis: Oregon State University Press.

Rybczynski N, Dawson, M.R., Tedford, R.H. 2009. A semi-aquatic Arctic mammalian carnivore from the Miocene epoch and origin of Pinnipedia. *Nature* 458:1021–24.

Sarich, V.M., 1969. Pinniped phylogeny. *Systematic Zoology* 18, 416–422.

Sanfelice, D., de Freitas, T.R.O. 2008. A Comparative Description of Dimorphism in Skull Ontogeny of *Arctocephalus australis*, *Callorhinus ursinus*, and *Otaria byronia* (Carnivora: Otariidae), *Journal of Mammalogy*, Volume 89(2):336–346.

Savage, R.J.G. 1957. The anatomy of Potamotherium an Oligocene lutrine. *Proc. Zool. Soc. Lond.* 129:151–244.

Schasse, H. W. 2003. Geologic map of the Washington portion of the Cape Flattery 1:100,000 quadrangle: Washington Division of Geology and Earth Resources Open File Report 2003-5, 1 sheet, scale 1:100,000.

Schmidt-Kittler, N. 1981. Zur Stammesgeschichte der marderverwandten Raubtiergruppen (Musteloidea, Carnivora). Eclogae Geol. Helv. 74, 753–801.

Schreer, J.F., and Kovacs, K.M. 1997. Allometry of diving capacity in air-breathing vertebrates. *Can. J. Zool.* 75: 339-358.

Siddall, M.E. 2002. Measures of Support. In: DeSalle, R., Giribet, G., Wheeler, W. (eds) *Techniques in Molecular Systematics and Evolution. Methods and Tools in Biosciences and Medicine.* Birkhäuser, Basel.

Sivertsen, E. 1954. A survey of the eared seals (Family Otariidae) with remarks on the Antarctic seals collected by M/K “Norvegia” in 1928-1929. Det Norske Vidensk.-Akad. Oslo 36:1-76.

Snavely, P., Niem, A., Pearl, J. 1978. Twin River Group (Upper Eocene to Lower Miocene) defined to include the Hoko River, Makah, and Pysht Formations, Clallam County, Washington. In Sohl, N., and Wright, W. (ed.) *Changes in Stratigraphic Nomenclature by the U.S. Geological Survey, 1977*. Geological Survey Bulletin 1457A:111-20.

Stirton, R.A. 1960. A marine carnivore from the Clallam Miocene Formation, Washington. Its correlation with nonmarine faunas. University of California Publications in Geological Sciences 36:345-368.

Tedford, R.H. 1976. Relationships of pinnipeds to other carnivores (Mammalia). *Syst. Zool.* 25:363–74.

Tedford, R.H., Barnes, L.G., and Ray, C.E. 1994. The Early Miocene Littoral Ursoid Carnivoran *Kolponomos*: Systematics and Mode of Life. In: Contributions in marine mammal paleontology honoring Frank C. Whitmore, Jr. *Proceedings of the San Diego Society of Natural History* 29:11-32.

Velez-Juarbe, J. 2017. Eotaria citrica, sp. nov., a new stem otariid from the “Topanga” formation of Southern California. PeerJ 5:e3022

Wang, X. M., McKenna, M. C., and Dashzeveg, D. 2005. *Amphicticeps* and *Amphicynodon* (Arctoidea, Carnivora) from Hsanda Gol Formation, central Mongolia, and phylogeny of basal arctoids with comments on zoogeography. Am. Mus. Novit. 3483, 1–57

Wyss, A.R. 1987. The walrus auditory region and monophyly of pinnipeds. *American Museum Novitates* 2871: 1-31.

Wyss, A.R. 1989. Flippers and pinniped phylogeny: has the problem of convergence been overrated? *Marine Mammal Science.* 5(4): 343-360.

Wyss, A.R. and Flynn, J.J. 1993. A phylogenetic analysis and definition of the Carnivora, Pp. 32-52 in Mammal phylogeny: Placentals (F. S. Szalay, M. J. Novacek and M. C. McKenna, eds.). Springer-Verlag, New York, NY.

Appendix

Appendix 1. Cranial measurements of basal pinnipedimorph holotype specimens in mm.

Measurements (mm)	***Pinnarctidion cf. bishopi*** SDNHM 146624	***P. bishopi*** UCMP 86334	***P. rayi*** USNM 314325	***Pteronarctos goedertae*** LACM 123883	***Enaliarctos mealsi*** LACM 4321	***E. mitchelli*** LACM 127816	***E. barnesi*** USNM 314295	***E. emlongi*** USNM 250345	***E. tedfordi*** USNM 206273
Cranium Length	>142		189.7	196.8				228.0	
Postpalatal Length		80.5	83.1	93.3	92.5			100.8	100.0
Length of toothrow, C to M2	52.4		66.1	69.7		63.8	69.3	78.2	
Width palate across anterior root of P4	35.0	44.0	41.0	37.2	37.9	30.7	49.7	56.4	52.0
Width rostrum across canines	33.0		38.1	47.9		38.1	58.4	55.4	
Transverse diameter infraorbital foramen		7.2	7.0	12.6			9.8	10.9	9.7
W. zygomatic root of maxilla		16.6	15.8	12.5	15.5	13.2	14.9	16.4	15.3

Basion to anterior edge of zygomatic root		130.2	126.7	137.6				152.6	142.9
Width across zygomatic arches	92.2	104.0	103.7	117.5	134.0			126.0	123.7
Auditory W.	75.6	82.6	72.4	76.9				87.8	91.9
Mastoid W.	?	90.6	84.4	105.2				103.1	105.8
Greatest width across occipital condyles	?	49.0	44.0	52.3	45.3			51.1	53.7
Greatest width foramen magnum	23.6	24.1	20.4	25.3	23.6			21.1	25.7
Greatest height foramen magnum	22.8	14.7	10.4	16.3	16.7			20.4	16.0
Greatest width nares	20.8		22.1	27.9		30.1	37.2	32.3	
Greatest height nares	22.4					27.0			
Least width across interorbital constriction	19.9	26.1	22.5	22.5	31.5	19.7	29.0	22.3	21.1

Width across antorbital processes	33.0	36.8		53.7		41.5	56.3	42.4	43.2
Width across supraorbital processes	24.9	26.3	25.0	34.6	38.0	28.8	40.1	29.0	28.2
Width between infraorbital foramina	43.0	41.0	44.7	53.5			57.0	59.3	59.0
Width of braincase at anterior edge of glenoid fossa	58.7	59.0	59.9	64.8	59.4			66.6	63.8

Appendix 2. List of specimens included in phylogenetic analysis

Taxon	Specimen number	Publication/Source
Canis lupus	IMNH R-884	IMNH
Ursus arctos	MVZ 46637	MVZ
Kolponomos clallamensis	LACM 131148	Stirton, 1960
Neovison vison	IMNH R-108	IMNH
Enhydra lutris	UWBM-38677	IMNH
Lontra canadensis	IMNH R-767	IMNH
Potamotherium valletoni	SG M11718	Savage, 1957
Puijila darwini	NUFV 405	Rybczynski 2009

Phoca vitulina	MVZ 153264	MVZ
Monachus monachus		
Erignathus barbatus	MVZ 124015	MVZ
Odobenus rosmarus	MVZ 125566	MVZ
Zalophus californianus	MVZ 125503	MVZ
Callorhinus ursinus	MVZ 175109	MVZ
Pinnarctidion cf. bishopi	SDNHM 146624	This study
Pinnarctidion bishopi	UCMP 86334	Barnes, 1979
Pinnarctidion rayi	USNM 314325	Berta, 1994a
Pteronarctos goedertae	LACM 123883	Barnes, 1989
Enaliarctos mealsi	LACM 4321	Mitchell and Tedford, 1973
Enaliarctos barnesi	USNM 314295	Berta, 1991
Enaliarctos emlongi	USNM 250345	Berta, 1991
Enaliarctos tedfordi	USNM 206273	Berta, 1991
Enaliarctos mitchelli	UCMP 100391	Barnes, 1979
Thalassoleon mexicanus	IGCU 902	Repenning and Tedford, 1977
Devinophoca claytoni	Z14523	Koretsky and Holec, 2002
Allodesmus kernensis	LACM 4320	Mitchell, 1966
Desmatophoca oregonensis	LACM 144452	Condon, 1906
Imagotaria downsi	USNM 23858	Mitchell, 1968
Proneotherium reppeningi	USNM 205334	Kohno et al., 1995
Gomphotaria pugnax	LACM 121508	Barnes and Raschke, 1991

Appendix 3. List of characters used in phylogenetic analysis.

Rostrum

1. Premaxilla-nasal contact. Deméré and Berta (2002: 1), B+C (2018: 1), Berta+Wyss (1994: 1)
0= <40% nasal length, no frontal contact
1= 40-60% total nasal length, no frontal contact
2= extensive contact or broadly sutured internally

2. Nasal-frontal suture. Deméré & Berta (2002: character 2)
0= nasals intrude between frontal
1= transverse
2= frontal intrudes between nasals

3. Ascending process of premaxilla-maxilla suture.
0= visible laterally along entire length
1= dips into nasal aperture

4. Posterior termination of nasals.
0= at or near frontal-maxillary contact
1= posterior to frontal-maxillary contact, nasals narrow greatly posteriorly

5. Anterior narial opening.
0= circular (subequal height/width)
1= ovoid horizontally (wider than dorsoventrally tall)
2= ovoid vertically (dorsoventrally taller than wide)

6. Nasal anterior margin.
0= excavated, nasal suture dips ventrally into naris
1= projecting, nasal suture projects anteriorly
2= w-shaped or transverse, nasal suture projects slightly anteriorly and ventrally

7. Prenarial process of premaxilla.
0= absent/indistinct
1= prominent, protrudes dorsal and anterior to alveolar margin

8. Nasolabialis fossa.
0= present
1= absent

Orbits

9. Maxilla contribution to the orbital wall.
0= no contribution
1= minor contribution
2= significant contribution

10. Antorbital process.
0= absent or indistinct
1= small rounded ridge
2= prominent, continuous with dorsal root of zygoma
3= prominent, distinct from zygoma

11. Supraorbital processes of frontals.
0= prominent, forms a point
1= reduced, forms a blunt ridge
2= absent or indistinct

12. Orbital vacuities.
0=absent
1=present

13. Lacrimal bone.
0= distinct
1= fused to maxilla or absent

14. Lacrimal foramen.
0= present
1= absent

15. Interorbital constriction.
0= thinnest at posterior end
1= relatively even thickness
2= thinnest at anterior end

16. Supraorbital process position.
0= closer to anterior orbital margin
1= equidistant to orbital and braincase margin
2= closer to expansion of braincase

Zygomatic arch

17. Infraorbital foramen shape.
0= small, slit-like
1= near-circular with no dorsal or ventral expansion
2= triangular with dorsomedial corner elongate
3= triangular with ventromedial corner elongate

18. Squamosal-jugal articulation.
0= splint-like, contact posterior to postorbital process
1= mortised, zygomatic process of squamosal fits into notch in postorbital process of jugal
2= mortised, zygomatic process of squamosal greatly expanded dorsoventrally

19. Ventral portion of anterior zygoma.
0= more dorsally placed, steeply inclined anteriorly
1= lower on skull and flatter

20. Posterior portion of zygomatic root of maxilla joins palate.
0= level with or posterior to M2
1= level with or posterior to M1
2= anterior to M1

21. Zygoma highest point of arching.
0= posteriorly, closer to expansion of braincase
1= continues arching posterior to postorbital process
2= at postorbital process, descends posteriorly

22. Zygoma shape.
0= relatively flat, not strongly arched
1= intermediately arched
2= strongly arched dorsally

23. Zygoma dorsoventral breadth.
0= thin
1= intermediate
2= broad

24. Orbital portion of zygoma length.
0= postorbital length greater than 2/3 of zygoma length
1= orbital length greater than 1/3 of zygoma length

25. Zygomatic transverse width.
0= widest point at approximate level of anterior border of the glenoid fossa, much wider than orbital width
1= widest anterior to glenoid fossa or posterior not significantly wider than orbital width

26. Jugal-maxillary suture.
0= jugal with anterodorsal and anteroventral splints
1= jugal with anterodorsal splint only
2= elongate anteroventral splint extends anteriorly to level of M1

27. Postorbital process of zygoma.
0= reduced, but still distinct
1= well-developed and pointed medially

2= indistinct, dorsal surface smooth and flush with zygoma

Braincase

28. Pseudosylvian sulcus.
0= absent, lateral wall of braincase smoothly convex
1= strongly developed

29. Anterolateral margin in dorsal view.
0= smoothly convex
1= forms a corner

30. Squamosal fossa.
0= undivided
1= divided

Palate

31. Embrasure pit between P4 and M1.
0= deep
1= shallow
2= absent

32. Embrasure pit between premolars.
0= absent
1= present

33. Incisive foramina position.
0= anterior to canines
1= level with canines
2= extend posterior to canines

34. Toothrow alignment.
0= parallel
1= slightly divergent
2= strongly divergent

35. Palatal transverse arching.
0= relatively flat
1= slightly arched
2= strongly arched

36. Palatine foramina.
0= single distinct pair
1= multiple distinct pairs with sulci

37. Palatine foramina position relative to toothrow.
0= terminate posterior to P4
1= terminate at or anterior to P4

38. Palatine process of maxilla posterior extension.
0= terminates at last molar
1= extends posteriorly from last molar
2= expanded as a shelf

39. Palatine process shape.
0= absent or indistinct
1= rounded or oblique (>90 degrees)
2= cornered or acute (<=90 degree vertex)

40. Palatal shelf ventral to posterior choana.
0= rounded/u-shaped
1= notched/v-shaped
2= median tuberosity projects posteriorly

41. Posterior choana transverse width.
0= narrow
1= wide

Pterygoid

42. Lateral wall of alisphenoid canal.
0= thick and well-developed
1= absent
2= thin

43. Pterygoid strut ventral profile.
0= thin
1= broad
2= very broad with lateral process

44. Pterygoid strut lateral margin.
0= relatively flat
1= concave
2= convex

Basicranium

45. Foramen rotundum.
0=within alisphenoid canal, separate from anterior lacerate foramen
1=within alisphenoid canal, merged with ALF
2=separate opening

46. Basioccipital lateral border with bulla.
0=bulla underlaps basioccipital
1=basioccipital bowed outward, abuts entotympanic

47. Flange of basioccipital.
0=absent
1=mildly flared
2=significantly flared

48. Depressions for rectis capitis muscle.
0=present
1=present with tuberosities for inferior petrosal venous sinus
2=insignificant or absent

49. Posterior lacerate foramen.
0=unenlarged
1=enlarged
2=anteriorly enlarged medial to basioccipital

50. Posterior carotid canal position relative to PLF.
0=posteriorly placed, opens into same fossa as PLF at posterior wall of bulla
1=posteriorly placed, does not open into same fossa as PLF
2=anteriorly placed, canal shortened

51. Postglenoid foramen.
0=present and large
1=vestigial or absent

52. Retroarticular process (postglenoid process).
0=medial prominence
1=reduced or indistinct
2=prominent with minimal directional bias

53. Articular tubercle (preglenoid process).
0=lateral prominence
1=reduced or indistinct
2=prominent with minimal directional bias

54. Mastoid process.
0=present
1=reduced or indistinct
2=enlarged

55. Paroccipital process.
0=present

1=reduced or indistinct
2=enlarged

56. Mastoid-paroccipital association.
0=mastoid more associated with nuchal crest, connected to PO by discontinuous ridge
1=more associated with PO, connected by well-developed ridge

Tympanic bullae

57. Petrosal visibility.
0=not visible in posterior lacerate foramen
1=visible through posterior lacerate foramen

58. Inflation.
0=ectotympanic flat with minimal inflation
1=only ectotympanic significantly inflated
2=ectotympanic and caudal entotympanic moderately inflated
3=ento and ecto greatly inflated and bulbous

59. Dorsal region of petrosal.
0=unexpanded
1=expanded

60. Pit for tensor tympani.
0=present
1=absent

61. Pit for tympanohyal.
0=closely associated with stylomastoid foramen
1=separated, posteromedial
2=separated, anterolateral

62. Internal auditory meatus.
0=present, canals vestibulocochlear and facial nerves in single foramen
1=present, canals incipiently separated
2=absent, canals completely separated into two foramina

Ear ossicles

63. Auditory ossicles.
0=small
1=enlarged

64. Round window.
0=small
1=enlarged

65. Basal whorl of scala tympani.
0=small
1=enlarged

66. Basal cochlear whorl.
0=posterolateral to long axis of skull
1=transversely directed

67. Cochlear aqueduct.
0=small
1=enlarged

68. Canal for cochlear aqueduct.
0=separate from round window
1=merged with round window

69. External cochlear foramen.
0=opens into middle ear
1=opens externally

70. Muscular process of malleus.
0=present
1=reduced
2=absent

71. Processus gracilis (rostral process) and anterior lamina (osseous lamina) of malleus.
0=unreduced
1=reduced

Occipital

72. Foramen magnum.
0=ovoid horizontally (width >> height)
1=round

Incisors

73. I3 lingual cingulum.
0=present
1=absent

74. I3 size and shape.
0=moderately larger than I1-2
1=similar in size to I1-2
2=much larger (>2x dimensions of I1-2), and canine-like

75. I1.
0=present
1=absent

76. Incisor roots.
0=transversely compressed
1=round

77. Incisor transverse grooves.
0=present
1=absent

78. Incisor row shape.
0=curved
1=straight

Canines

79. Posterior crista.
0=sharply defined
1=weak or absent
2=canines greatly enlarged

Premolars

80. P1-3 cingula.
0=narrow smooth lingual cingulum
1=narrow cuspate lingual cingulum
2=well-developed cuspate cingulum
3=no cingula

81. P1 lingual cingulum.
0=absent
1=present

82. P1 labial cingulum.
0=absent
1=present

83. P1 cingular heel.
0=present
1=absent

84. P1 size relative to other premolars.
0=smaller

1=similar in size (if only one rooted, that root is larger than other premolar roots)
2=absent

85. P1 position along toothrow.
0=parallel
1=offset medially

86. P2 metacone.
0=cingular heel
1=absent
2=accessory cusp distinct from cingular heel

87. P2 root.
0=double
1=single

88. P3 metacone.
0=absent or small
1=prominent cingular heel
2=accessory cusp distinct from cingular heel

89. P3 lingual cingulum.
0=absent
1=present
2=posterolingual shelf

90. P3 root.
0=double
1=single

91. P3 protocone shelf.
0=absent
1=small
2=large

92. P4 protocone shelf.
0=large
1=small
2=absent

93. P4 protocone position.
0=anteriorly, adjacent to paracone
1=intermediate, forming an equilateral triangle between paracone and metacone
2=posteriorly, forming right-triangle adjacent to metacone
3=absent

94. P4 roots.
0=triple
1=double, posterior bilobed
2=double, no bilobes
3=single

95. P4 paracone.
0=simple crest
1=accessory cusps present

96. P4 metacone.
0=large
1=reduced
2=absent

97. P4 contact with M1.
0=contacts M1
1=does not contact M1

Molars

98. M1 size compared to P4.
0=similar in size or M1 slightly larger
1=reduced in size
2=molars and premolars generally homodont

99. M1 roots.
0=triple
1=double, posterior bilobed
2=double, no bilobes
3=single

100. M1 accessory cusps.
0=hypocone, paracone, or other cusps present
1=no hypocone or paracone analogs

101. M1 protocone shelf and basin.
0=broad, posteromedially placed
1=cingulum instead of shelf, restricted basin
2=reduced basin bordered by shelf
3=both absent

102. M1 metacone vs. paracone height.
0=paracone higher than metacone
1=equal
2=metacone higher

103. M2 roots.
0=triple
1=double
2=single
3=absent

Appendix 4. List of synapomorphies according to parsimony Tree 1.

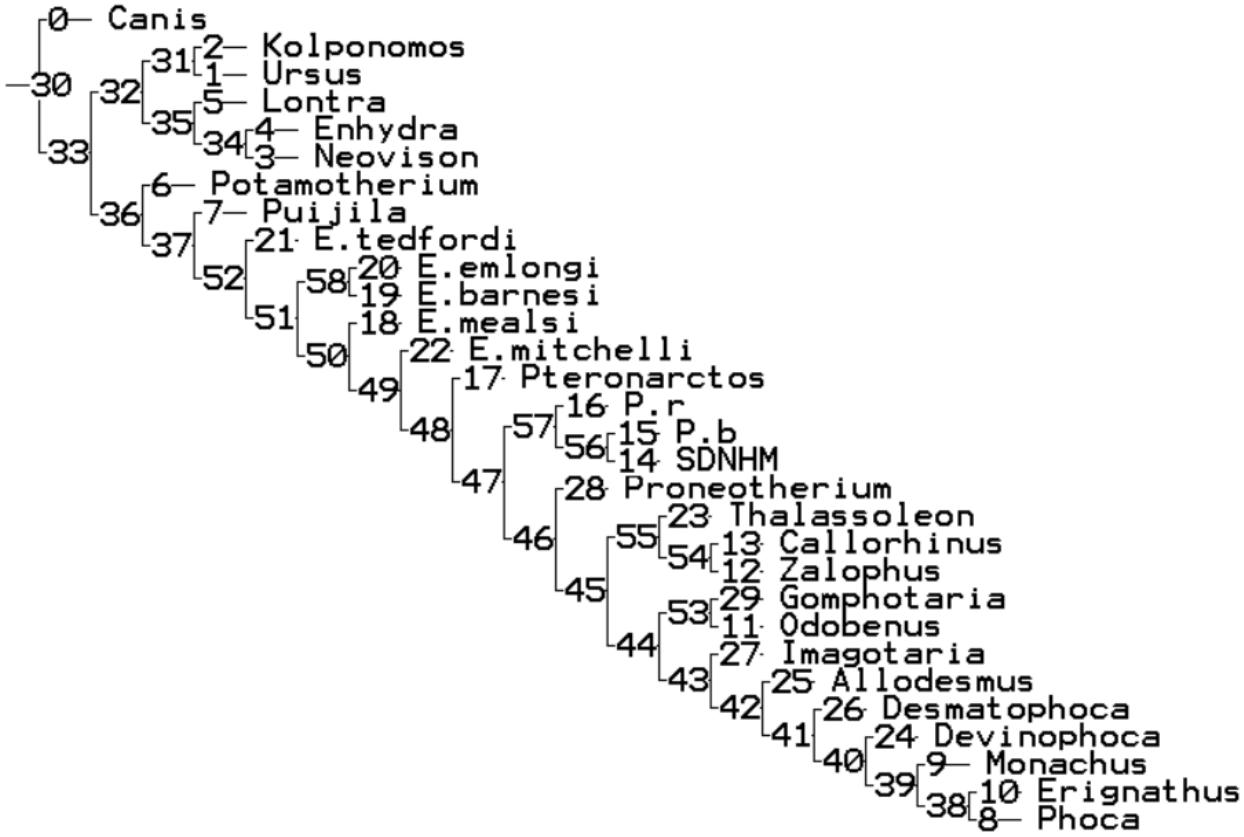

1. *Ursus arctos*
   26, 0→1 jugal with anterodorsal splint only
   51, 0→1 preglenoid process reduced
   55, 0→2 paroccipital process enlarged
   72, 0→1 foramen magnum round
   80, 0→1 narrow cuspate cingula
   101, 0→1 M1 protocone shelf absent, only cingulum present

2. *Kolponomos clallamensis*
   5, 0→2 anterior narial opening higher than wide
   7, 0→1 prenarial process of premaxilla prominent
   11, 0→1 supraorbital process reduced
   23, 1→2 zygomatic arch dorsoventrally broad
   25, 0→1 zygomatic widest anterior to glenoid fossa
   33, 1→2 incisive foramina extend posterior to canines
   74, 0→2 I3 much larger than other incisors
   103, 0→1 double rooted M2

3. *Neovison vison*
   8, 0→1 nasolabialis fossa absent
   36, 0→1 multiple pairs of palatine foramina with sulci
   45, 1→2 foramen rotundum has separate opening
   58, 0→1 only ectotympanic inflated
   92, 0→1 small P4 protocone shelf

4. *Enhydra lutris*
   3, 0→1 ascending process of premaxilla dips into nasal aperture
   6, 2→0 excavated nasal anterior margin
   11, 0→1 supraorbital process reduced
   20, 2→1 zygomatic root level with M1
   21, 1→0 zygoma highest point of arching more posterior
   31, 0→1 shallow embrasure pit
   41, 0→1 wide choana
   93, 0→1 P4 protocone positioned intermediately
   102, 1→0 M1 paracone higher than meta

5. *Lontra canadensis*
   10, 0→2 antorbital process prominent, continuous with dorsal root of zygoma
   40, 0→2 palatal shelf has median tuberosity
   43, 1→2 pterygoid strut very broad
   80, 0→2 well developed cuspate cingula

6. *Potamotherium valletoni*
   25, 0→1 zygoma widest anterior to glenoid fossa
   30, 0→1 divided squamosal fossa
   42, 0→1 alisphenoid canal absent
   85, 0→1 P1 offset medially
   86, 0→2 P2 accessory cusps

7. *Puijila darwini*
   31, 0→1 shallow embrasure pit
   34, 1→0 toothrow parallel
   48, 0→1 depression present with tuberosities

62, 0→1 IAM present, incipiently separated
72, 0→1 foramen magnum round
79, 0→1 canine crista absent
82, 0→1 P1 labial cingulum present
88, 2→1 P3 cingular heel

8. *Phoca vitulina*
   35, 0→1 palate slightly arched
   49, 1→2 PFL anteriorly enlarged medial to basioccipital
   56, 0→1 mastoid associated with paroccipital
   78, 0→1 straight incisor row
   84, 0→1 P1 similar in size

9. *Monachus monachus*
   33, 2→1 incisive foramina level with canines
   46, 0→1 basioccipital bowed outward
   72, 0→1 foramen magnum round
   73, 1→0 I3 lingual cingulum present
   75, 0→1 I1 absent

10. *Erignathus barbatus*
    6, 2→0 excavated anterior nasal margin
    7, 0→1 prenarial process prominent
    25, 1→0 zygoma widest near glenoid fossa
    26, 1→0 jugal with anterodorsal and anteroventral splints
    48, 2→0 depression for rectis capitis
    50, 1→0 carotid canal posteriorly placed, opens into same fossa as PLF
    85, 1→0 P1 in line with toothrow
    96, 1→2 P4 metacone absent

11. *Odobenus rosmarus*
    6, 0→2 transverse anterior nasal margin
    36, 0→1 multiple distinct pairs of palatine foramina
    39, 1→2 palatine process cornered
    41, 0→1 wide choana
    54, 0→2 mastoid process enlarged
    80, 1→3 no cingula
    92, 1→2 absent P4 protocone shelf
    103, 2→3 M2 absent

12. *Zalophus californianus*
    83, 0→1 P1 cingular heel absent
    96, 1→2 P4 metacone absent

13. *Callorhinus ursinus*
    15, 0→1 interorbital constriction relatively even thickness

18, 0→1 mortised squamosal-jugal articulation
22, 0→2 zygoma strongly arched dorsally
30, 0→1 divided squamosal fossa
33, 2→1 incisive foramina level with canines
47, 1→2 flange of basioccipital significantly flared
74, 2→0 I3 moderately larger

14. SDNHM 146624
23, 1→2 dorsoventrally broad zygoma
34, 1→2 palate strongly divergent
53, 1→0 preglenoid process with lateral prominence
72, 0→1 foramen magnum round
95, 0→1 accessory cusp on P4 crest
99, 1→2 M1 double rooted with no bilobe

15. *Pinnarctidion bishopi*
35, 1→0 palate relatively flat

16. *Pinnarctidion rayi*
1, 2→0 shorter premaxilla-nasal contact
46, 1→0 bulla medially expanded, underlaps basioccipital
48, 1→0 rectis capitis depression present with no tuberosities
57, 0→1 petrosal visible through PLF

17. *Pteronarctos goedertae*
13, 1→0 distinct lacrimal bone
14, 1→0 lacrimal foramen present
22, 0→1 zygoma intermediately arched
37, 0→1 palatine foramina terminate at or anterior to P4

18. *Enaliarctos mealsi*
22, 0→2 zygoma strongly arched dorsally
36, 0→1 multiple pairs of palatine foramina
40, 0→1 palatal shelf v-shaped
53, 1→2 preglenoid process prominent with minimal directional bias

19. *Enaliarctos barnesi*
23, 0→2 zygomatic arch dorsoventrally broad
34, 1→0 toothrow parallel
39, 1→2 palatine process cornered
82, 0→1 P1 labial cingulum present
83, 0→1 P1 cingular heel absent
88, 2→0 P3 metacone absent
91, 1→2 large P^3 protocone shelf

20. *Enaliarctos emlongi*

36, 0→1 multiple palatine foramina
80, 0→2 well developed cuspate cingula

21. *Enaliarctos tedfordi*
27, 1→0 reduced postorbital process of zygoma
55, 0→2 paroccipital process enlarged
80, 0→2 well developed cuspate cingula
93, 0→1 P4 protocone posteriorly placed

22. *Enaliarctos mitchelli*
6, 2→0 anterior nasal margin excavated
27, 1→0 postorbital process reduced
39, 1→2 palatine process cornered

23. *Thallasoleon mexicanus*
22, 2→1 zygoma intermediately arched
99, 3→2 M1 roots double, no bilobe

24. *Devinophoca claytoni*
4, 1→0 posterior termination of nasals at or near frontal-maxillary contact
8, 1→0 nasolabialis fossa present
89, 2→1 P3 lingual cingulum, no shelf
94, 2→1 P4 root double with posterior bilobe
101, 3→2 M1 protocone basin bordered by shelf

25. *Allodesmus kernensis*
15, 0→1 interorbital constriction relatively even thickness
27, 1→2 postorbital process indistinct from zygoma
42, 0→2 alisphenoid canal thin
79, 0→1 canine crista absent
80. 2→3 no cingula
92, 1→2 absent P4 protocone shelf

26. *Desmatophoca oregonensis*
12, 1→0 orbital vacuities absent
17, 3→1 infraorbital foramen near circular
18, 02→1 mortised squamosal-jugal articulation
21, 2→1 zygoma continues arching posterior to postorbital process
33, 2→1 incisive foramen level with canines
35, 2→1 palate slightly arched
36, 0→1 multiple palatine foramina
78, 0→1 straight incisor row

27. *Imagotaria downsi*
12, 1→0 orbital vacuities absent
34, 1→0 toothrow parallel

38, 2→1 palatine process extends posteriorly, no shelf
99, 3→2 M1 roots double, no bilobe

28. *Proneotherium repenningi*
    50, 0→1 carotid canal posteriorly placed, does not open into same fossa as PLF
    54, 0→2 mastoid process enlarged
    86, 0→2 P2 accessory cusps
    88, 1→2 P3 accessory cusps present
    95, 0→1 P4 paracone with accessory cusps

29. *Gomphotaria pugnax*
    4, 0→1 nasals terminate posterior to frontal-maxillary contact, narrow greatly posteriorly
    24, 1→0 postorbital length greater than 2/3 of zygoma length
    53, 1→ preglenoid process laterally prominent
    58, 0→1 only ectotympanic inflated

30. Caniformia
    No synapomorphies

31. Ursidae
    6, 2→1 nasal suture projects anteriorly
    21, 1→0 zygoma highest point of arching near position of glenoid fossa
    31, 0→2 no embrasure pit
    37, 1→0 palatine foramina terminate posterior to P4
    46, 0→1 basioccipital bowed outward
    92, 0→1 small P4 protocone shelf
    93, 0→2 P4 protocone positioned posteriorly

32. Ursidae + Mustelidae
    38, 1→0 palatine process terminates at last molar
    43, 0→1 pterygoid strut broad
    44, 0→1 pterygoid strut concave
    58, 2→0 ectotympanic flat
    83, 0→1 P1 cingular heel absent
    102, 0→1 M1 metacone and paracone equal height

33. Arctoidea
    No synapomorphies

34. *Enhydra + Neovison*
    16, 0→1 supraorbital process equidistant to braincase and orbital margin
    48, 0→2 no depression for rectis capitis
    79, 0→1 canine crista absent
    84, 0→2 P1 absent

35. Mustelidae
    23, 1→0 zygoma dorsoventrally thin
    30, 0→1 divided squamosal fossa
    42, 0→1 alisphenoid canal absent
    45, 0→1 foramen rotundum within alisphenoid canal, merged with ALF
    55, 0→1 paroccipital process reduced
    85, 0→1 P1 offset medially
    103, 0→3 absent M2

36. *Potamotherium* + other pinnipedimorphs
    11, 0→1 supraorbital process reduced
    53, 0→1 preglenoid process reduced
    71, 0→1 reduced processus gracilis of malleus
    88, 0→2 P3 accessory cusps
    103, 0→2 single rooted M2

37. *Puijila* + other pinnipedimorphs
    46, 0→1 basioccipital bowed outward
    56, 0→1 mastoid associated with paroccipital process
    64, 0→1 enlarged round window
    67, 0→1 large cochlear aqueduct

38. *Phoca* + *Erignathus*
    5, 0→2 anterior narial opening higher than wide
    15, 0→2 interorbital constriction thinnest at anterior end
    22, 2→1 zygoma intermediately arched
    39, 0→2 palatine process cornered
    47, 1→0 flange of basioccipital absent
    54, 0→1 mastoid process reduced
    79, 0→1 canine crista absent
    80, 1→3 no cingula
    81, 1→0 absent P1 lingual cingulum
    83, 0→1 absent P1 cingular heel
    89, 2→0 absent P3 lingual cingulum
    91, 1→0 absent P3 protocone shelf
    92, 1→2 absent P4 protocone shelf
    99, 1→2 homodont molars

39. (*Phoca* + *Erignathus*) + *Monachus*
    11, 1→2 supraorbital process indistinct
    35, 2→0 palate relatively flat
    41, 0→1 wide choana
    99, 1→2 M1 roots double no bilobe

40. ((*Phoca* + *Erignathus*) + *Monachus*) + *Devinophoca*
    19, 1→0 ventral portion of anterior zygomatic root more dorsally placed

25, 0→1 zygoma widest anterior to glenoid fossa
26, 2→1 jugal with anterodorsal splint only
34, 1→2 toothrow strongly divergent
39, 1→0 palatine process absent
55, 2→1 paroccipital process reduced
56, 1→0 mastoid more associated with nuchal crest
80, 2→1 narrow cuspate cingula
90, 1→0 double P3 root
103, 2→3 M2 absent

41. Phocids + *Desmatophoca*
6, 0→2 nasal anterior margin transverse or w-shaped
62, 1→2 IAM absent, canals separate
87, 1→0 double P2 root
99, 3→1 M1 roots double, bilobed

42. (Phocids + *Desmatophoca*) + *Allodesmus*
1, 2→1 premaxilla contacts 40-60% length of nasal
4, 0→1 nasals terminate posterior to frontal-maxillary contact, narrow greatly posteriorly
7, 1→0 prenarial process absent
10, 2→1 antorbital process small, rounded ridge
26, 0→2 jugal-maxillary suture elongate anteroventral splint extends anteriorly to level of M1
43, 2→1 pterygoid strut broad
46, 1→0 bulla underlaps

43. ((Phocids + *Desmatophoca*) + *Allodesmus*) + *Imagotaria*
59, 0→1 dorsal region of petrosal expanded
80, 0→2 well developed cuspate
cingula

44. Odobenids + (((Phocids + *Desmatophoca*) + *Allodesmus*) + *Imagotaria*)
29, 1→0 anterolateral margin of braincase smoothly convex
57, 0→1 petrosal visible through PLF
63, 0→1 enlarged auditory ossicles
68, 0→1 canal for cochlear aqueduct merged with round window

45. Crown Pinnipedia
10, 1→2 antorbital process prominent, continuous with zygoma
21, 1→2 highest zygomatic arching at postorbital process
31, 1→2 no embrasure pit
39, 2→1 palatine process rounded
73, 0→1 I3 lingual cingulum absent
94, 1→23 P4 roots double or single
99, 1→3 M1 single rooted

101, 2→3 M1 protocone shelf absent

46. *Proneotherium* + Pinnipedia
    8, 0→1 nasolabialis fossa absent
    12, 0→1 orbital vacuities present
    55, 0→2 paroccipital process enlarged
    58, 2→0 ectotympanic flat with minimal inflation
    74, 0→2 I^3 much larger than other incisors
    96, 0→1 P^4 metacone reduced

47. *Pinnarctidion* + other pinnipedimorphs
    38, 1→2 palatine process expanded as a shelf
    92, 0→1 small P4 protocone shelf

48. *Pteronarctos* + other pinnipedimorphs
    20, 1→0 posterior portion of zygomatic root level with or posterior to M2
    21, 2→1 zygoma continues arching posterior to postorbital process
    23, 0→1 intermediate zygoma dorsoventral breadth
    31, 0→1 shallow embrasure pit between P4 and M1
    94, 0→1 P4 double rooted, posterior bilobed

49. *Enaliarctos mitchelli* + other pinnipedimorphs
    19, 0→1 ventral portion of zygoma lower on skull and flatter
    39, 1→2 palatine process sharply cornered

50. *Enaliarctos mealsi* + other pinnipedimorphs
    17, 1→3 IOF triangular with ventromedial corner elongate
    24, 0→1 orbital length greater than 1/3 of zygoma
    48, 0→1 depression for rectis capitis present with tuberosities
    54, 2→0 mastoid process present, not enlarged

51. *Enaliarctos emlongi* and *E. barnesi* + other pinnipedimorphs
    21, 1→2 zygoma highest arching at postorbital process
    61, 0→1 pit for tympanohyal separated, posteromedially placed
    89, 1→2 P3 posterolingual shelf

52. *Enaliarctos tedfordi* + other pinnipedimorphs
    5, 0→1 narial opening ovoid horizontally
    14, 0→1 lacrimal foramen absent
    17, 2→1 IOF near circular
    20, 2→1 zygomatic root level with or posterior to M1
    23, 1→0 zygoma dorsoventrally thin
    28, 0→1 strongly developed pseudosylvian sulcus
    29, 0→1 anterolateral margin of braincase forms a corner
    43, 0→1 pterygoid strut broad
    52, 0→2 postglenoid process prominent with minimal direction

91, 0→1 small P3 protocone shelf
98, 0→1 M1 reduced in size
99, 0→1 M1 roots double, posterior bilobed instead of 3

53. *Odobenus* + *Gomphotaria*
19, 1→0 ventral portion of anterior zygoma more dorsally placed
55, 2→0 paroccipital process present
75, 0→1 I1 absent
79, 0→2 canines greatly enlarged
81, 0→1 P1 cingular heel absent
86, 0→1 P2 metacone absent
96, 1→2 P4 metacone absent

54. Callorhinus + *Zalophus*
6, 0→2 nasal anterior margin w-shaped or transverse
34, 1→0 toothrow parallel
38, 2→1 palatine process extends, but no shelf
39, 1→0 palatine process absent
86, 0→1 P2 metacone absent

55. *Thalassoleon* + (*Callorhinus* + *Zalophus*)
1, 2→1 premaxilla contact 40-60% length of nasal
2, 01→2 frontal intrudes between nasals
11, 1→0 supraorbital process prominent, forms a point
16, 0→1 supraorbital process equidistant to orbital and braincase margin
20, 0→1 posterior portion of zygomatic root level with or posterior to M1
43, 2→0 pterygoid strut thin
62, 1→0 IAM present, merged
80, 0→1 narrow cuspate cingula
92, 1→2 absent P4 protocone shelf

56. *Pinnarctidion bishopi* + SDNHM 146624
14, 1→0 lacrimal foramen present
36, 0→1 multiple palatine foramina
39, 2→1 oblique palatine process
58, 2→1 only ectotympanic significantly inflated
96, 0→1 P4 metacone reduced
102, 0→2 M1 metacone higher than paracone

57. Pinnarctidion
6, 0→2 w-shaped anterior nasal margin
15, 0→1 interorbital constriction even thickness
16, 0→1 postorbital constriction relatively equal length to interorbital
18, 0→1 mortised squamosal-jugal
25, 0→1 zygoma widest anterior to glenoid fossa
41, 0→1 wide choana width

58. *Enaliarctos emlongi* + *E. barnesi*
    32, 0→1 embrasure pit between premolars
    40, 0→2 palatal shelf has median tuberosity